HRPK-1, a conserved KH-domain protein, modulates microRNA activity during *Caenorhabditis elegans* development

Li Li[1], Isana Veksler-Lublinsky[2], and Anna Y. Zinovyeva[1*]

[1] Division of Biology, Kansas State University, Manhattan, KS, USA

[2] Department of Software and Information Systems Engineering, Ben-Gurion University, Beer-sheva, Israel

*Corresponding author

Email: zinovyeva@ksu.edu

Running title: hrpk-1 regulates microRNA activity

Key words: microRNAs, KH domain, hrpk-1, hnRNPK

Abstract

microRNAs (miRNAs) are potent regulators of gene expression that function in diverse developmental and physiological processes. Argonaute proteins loaded with miRNAs form the miRNA Induced Silencing Complexes (miRISCs) that repress gene expression at the post-transcriptional level. miRISCs target genes through partial sequence complementarity between the miRNA and the target mRNA's 3' UTR. In addition to being targeted by miRNAs, these mRNAs are also extensively regulated by RNA-binding proteins (RBPs) through RNA processing, transport, stability, and translation regulation. While the degree to which RBPs and miRISCs functionally interact to regulate gene expression is likely extensive, we have only begun to unravel these functional interactions. An RNAi-based screen of putative ALG-1 Argonaute interactors has identified a role for a conserved RNA binding protein, HRPK-1, in modulating miRNA activity during *C. elegans* development. Here, we report the physical and genetic interaction between HRPK-1 and ALG-1/miRNAs. Specifically, we report the genetic and molecular characterizations of *hrpk-1* and its role in *C. elegans* development and miRNA-mediated target repression. We show that loss of *hrpk-1* causes numerous developmental defects and enhances the mutant phenotypes associated with reduction of miRNA activity, including those of *lsy-6, mir-35*-family, and *let-7*-family miRNAs. In addition to *hrpk-1* genetic interaction with these miRNA families, *hrpk-1* is required for efficient regulation of *lsy-6* target *cog-1*. We report that *hrpk-1* may play a role in miRNA processing but is not globally required for mature miRNA biogenesis or ALG-1/AIN-1 miRISC assembly and confirm HRPK-1 ability to co-precipitate with ALG-1. We suggest that HRPK-1 may functionally interact with miRNAs on multiple levels to enhance miRNA/miRISC gene regulatory activity and present several models for its activity.

Author summary

microRNAs are small non-coding RNAs that regulate gene expression at the post-transcriptional level. The core microRNA Induced Silencing Complex (miRISC), composed of Argonaute, mature microRNA, and GW182 protein effector, assembles on the target messenger RNA and inhibits translation or leads to messenger RNA degradation. RNA binding proteins interface with miRNA pathways on multiple levels to coordinate gene expression regulation. Here, we report identification and characterization of HRPK-1, a conserved RNA binding protein, as a physical and functional interactor of miRNAs. We confirm the physical interaction between HRPK-1, an hnRNPK homolog, and Argonaute ALG-1. We report characterizations of *hrpk-1* role in development and its functional interactions with multiple miRNA families. We suggest that HRPK-1 promotes miRNA activity on multiple levels in part by contributing to miRNA processing and by coordinating with miRISC at the level of target RNAs. This work contributes to our understanding of how RNA binding proteins and auxiliary miRNA cofactors may interface with miRNA pathways to modulate miRNA gene regulatory activity.

Introduction

Robust regulation of gene expression is essential for normal development and cellular homeostasis. microRNAs (miRNAs), small non-coding RNAs ~22nt in length, negatively regulate gene expression at the post-transcriptional level. miRNAs can act as developmental switches or can fine tune the expression of the target genes (for review, see [1], [2]). Processed miRNAs are loaded into their main protein cofactor, Argonaute (AGO), which then associates with members of the GW182 family of proteins, forming the microRNA Induced Silencing Complex (miRISC). Mature miRISCs bind to the target messenger RNAs (mRNAs) and repress their translation and/or destabilize the target mRNA [3], [4].

RNA binding proteins (RBPs) make up another class of post-transcriptional gene regulators. RBPs can affect miRNA gene-repressive activity in a variety of ways, including through miRNA processing [5] and mRNA co-targeting through mRNA processing, transport, localization, stability/degradation and mRNA translation regulation. A given mRNA bound by miRISC also serves as a platform for binding of additional RNA-interacting factors, and a few have been shown to associate with core miRISC and modulate its activity [6], [7], [8]. For example, NHL-2 and CGH-1 physically interact with miRISC and enhance the repression of miRNA target genes [7], a process regulated by casein kinase II [9] . Furthermore, many genes, including RNA binding proteins (RBPs), have been identified as genetic interactors of the *let-7* family of miRNAs [10], [11], [12], [13]. It remains unclear how many of them function as direct modulators of miRISC activity. Complementary to these approaches, we have previously sought to identify physical interactors of ALG-1, a miRNA-specific *C. elegans* Argonaute [14], hypothesizing that proteins that co-precipitate with ALG-1 include factors that modulate miRNA-induced gene repression. An RNAi-based screen of the putative ALG-1 co-factors has identified HRPK-1, a conserved homolog of human heterogeneous nuclear ribonucleoprotein K (hnRNPK), as a novel miRNA interactor that modulates activity of several

miRNAs. Here, we report the characterization of both physical and genetic interactions between HRPK-1 and miRNA-containing complexes.

Heterogeneous nuclear ribonucleoproteins (hnRNPs) form a large family of nucleic acid binding proteins with diverse functions in a wide range of cellular processes, including transcription, RNA processing, RNA transport, RNA stability, and translational repression [15]. They possess multiple domains and are thought to form modular complexes, increasing the diversity of the RNA/protein interactions [16]. Several hnRNPs have recently emerged as having roles in miRNA-mediated gene regulation [15]. Some are implicated in biogenesis of specific miRNAs [17], while others, such as hnRNP Q, appear to hinder miRNA activity by competing with key molecular effectors of miRISC [18]. KH domain proteins are a subclass of hnRNPs with similarly diverse functions [15]. These proteins contain the KH nucleic acid binding motifs, which were originally identified in heterogeneous nuclear ribonucleoprotein K (hnRNPK), with KH domain named for K homology [19]. KH domains are evolutionary conserved and are found in approximately 40 of human genes, and 27 of *C. elegans* genes. These nucleic acid binding motifs are 70 amino acids in size and can be present as a single domain or in multiple copies within a given protein [20], [19]. For example, Vigilin, a ribosome associated protein, contains 14 KH domains [21], [22]. It is thought that each KH domain can act as an independent binding module [23], although it is not currently clear if that holds true for all KH-containing proteins. Interestingly, a *C. elegans* homolog of the Vigilin gene, *vgln-1*, has been recently shown to cooperate with miRNAs to regulate gene expression [24].

Recent studies have implicated the human hnRNPK in miRNA-mediated gene repression. One study reports that hnRNPK may compete with multiple miRNAs for 3'UTR binding of their target gene, *PLK1* [25]. Such target binding competition puts hnRNPK in a role of a negative regulator of miRNA activity [25]. Other studies have placed hnRNPK in close physical proximity to miRNAs themselves, observing hnRNPK binding to miR-122 miRNA directly and potentially regulating its stability [26] or

binding near miR-122 target sites on target mRNAs [27]. The functional significance of these interactions has not yet been described. In *C. elegans,* two KH domain-containing proteins, GLD-1 and VGLN-1 have been shown to genetically and/or physically interact with miRNA machinery [28] and [24], respectively. The mechanism through which GLD-1 and VGLN-1 functionally interact with the miRNA pathways remains unclear.

We have previously identified HRPK-1(F26B1.2), an hnRNPK homolog, in ALG-1 Argonaute immunoprecipitates as a putative ALG-1 physical interactor [14]. Here, we report the characterization of *hrpk-1* as a functional miRNA interactor that modulates activity of several miRNAs. Loss of *hrpk-1* results in a number of developmental defects, including sterility, embryonic lethality, vulval bursting, loss of alae, and abnormal gonad formation. Genetic loss of HRPK-1 enhances miRNA reduction-of-function phenotypes, consistent with HRPK-1 functional requirement for wild type miRNA activity. We report that HRPK-1 is ubiquitously expressed throughout *C. elegans* development and localizes to both nuclei and cytoplasm in some tissues, while remaining strongly nuclear in others. We confirm that HRPK-1 co-precipitates ALG-1 by immunoprecipitation. Finally, while *hrpk-1* appears to be globally dispensable for miRNA biogenesis, it may play a role in processing of select miRNAs. HRPK-1 is not needed for ALG-1/AIN-1 miRISC assembly, suggesting that HRPK-1 may also functions at the level of miRNA target repression, especially in case of miRNAs whose processing does not depend on HRPK-1 activity.

Our data suggest that HRPK-1 may regulate miRNA activity by interacting with miRNA-associated protein complexes and modulating the efficacy of both mature miRNA processing and miRNA activity on target mRNAs. This furthers our understanding of how miRNAs may be regulated by or function in concert with RNA binding proteins. Our findings also demonstrate that RNA binding proteins may integrate distinct developmental and physiological signals with miRNA-mediated gene repression.

Results

To identify and characterize potential physical and functional interactions of HRPK-1 with miRISC components, we first generated a null allele in *hrpk-1.* A previously existing deletion allele of *hrpk-1, hprk-1(tm5522),* causes an in-frame deletion within the *hrpk-1* gene, resulting in production of a truncated HRPK-1 protein (Fig 1A-C). Using CRISPR/Cas9-based genome editing, we generated two independent null alleles of *hrpk-1, hrpk-1(zen15)* and *hrpk-1(zen17)* (Fig1A-C). Both alleles nearly completely or completely delete the *hrpk-1* locus (Fig 1A) and produce no HRPK-1 protein (Fig 1B-C). Since both null alleles produce a similar loss-of function phenotype (S1 Fig), we have designated the larger deletion, *hrpk-1(zen17)*, as the reference null allele for *hrpk-1* and used it in subsequent analyses.

ALG-1 Argonaute and HRPK-1 co-immunoprecipitate in a partially RNA dependent manner.

We have previously identified HRPK-1(F26B1.2) by immunoprecipitating *C. elegans* miRNA-specific Argonaute ALG-1 and analyzing the co-purified protein complexes by MudPIT proteomics [14], (Fig 1D). To confirm this physical interaction, we performed reciprocal IP using antisera generated against HRPK-1 and probed for the presence of ALG-1. We found that HRPK-1 IP co-precipitates ALG-1 (Fig 1E), consistent with HRPK-1 interaction with the miRNA machinery.

To determine whether HRPK-1/ALG-1 co-immunoprecipitation is RNA dependent, we performed the HRPK-1 IP in the presence of RNAse A (20μg/ml). Interestingly, incubation of lysates with RNAse A prior to and during HRPK-1 IP reduces but does not abolish ALG-1 co-precipitation with HRPK-1 (Fig 1E). This result suggests that while the ALG-1/HRPK-1 binding may in part depend on RNA, the two proteins may also be interacting directly, rendering the observed interaction partially RNAse A resistant (Fig 1E). The ALG-1/HRPK-1 interaction may be strengthened through RNA-protein interactions.

hrpk-1 is required for a number of developmental processes.

To determine what effects *hrpk-1* mutations have on animal development, we characterized gross morphological phenotypes of both *hrpk-1(tm5522)* and *hrpk-1(zen17)* mutants. We found that both alleles induce temperature sensitive sterility (Fig 2A), embryonic lethality (Fig 2B), and reduced brood size (Fig 2C). Both alleles also cause gonad formation defects (Fig 2D, E) and vulval bursting in day 3 or older adults (Fig 2F). We observed that almost in every instance, homozygous *hrpk-1(tm5522)* mutants exhibit more severe phenotypes than complete loss of *hrpk-1* (Fig 2A-C,G), with the exception of gonad morphology (Fig 2D,E) and vulval bursting (Fig 2F) defects. *hrpk-1(tm5522)* mutant animals also fail to produce adult alae approximately 40% of the time (Fig 2G). In addition, *hrpk-1* function appears to be maternally required for fertility (S2 Fig A), brood size (S2 Fig B), and embryonic viability (S2 Fig C). Specifically, *hrpk-1(zen17) [m-z-]* animals have increased defects compared to *hrpk-1(zen17) [m+z-]* in sterility (S2 Fig A), brood size (S2 Fig B), and embryonic lethality (S2 Fig C).

hrpk-1(tm5522) allele is antimorphic.

Our genetic analysis suggests that *hrpk-1(tm5522)* allele is weakly semi-dominant and antimorphic in nature (S2 Fig). Firstly, homozygous *hrpk-1(tm5522)* mutants almost always exhibit more severe phenotypes than *hrpk-1(zen17)* null animals (Fig 2A-C, G). Secondly, *hrpk-1(tm5522)/+ [m-z+]* animals carrying only a single copy of the wild type allele exhibited higher fertility defects and vulval bursting than *hrpk-1(zen17)/+ [m-z+]* animals (14% sterility versus 0%, respectively, S2 Fig A and D). Thirdly, *hrpk-1(tm5522)/+ [m+z+]* animals show a modest reduction in brood size (S2 Fig B) and embryonic lethality (S2 Fig C) and vulval bursting (S2 Fig D) not normally observed in wild type animals. Furthermore, animals carrying a single copy of maternally provided *hrpk-1(tm5522)* allele

(*hrpk-1(tm5522)*♀*/hrpk-1(zen17)*♂ produced by *hrpk-1(tm5522)* mothers and *hrpk-1(zen17)* fathers) exhibit higher rates of sterility (S2 Fig A), have smaller brood sizes (S2 Fig B), and higher embryonic lethality (S2 Fig C) than *hrpk-1(zen17) [m-z-]* animals lacking functional *hrpk-1* completely. Animals carrying a single copy of maternally provided *hrpk-1(tm5522)* allele (*hrpk-1(tm5522)*♀*/hrpk-1(zen17)*♂ also show more severe phenotypes than *hrpk-1(tm5522)*♂*/ hrpk-1(zen17)*♀ animals produced by *hrpk-1(tm5522)* fathers and *hrpk-1(zen17)* mothers (S2 Fig A-C), likely a result of both the antimorphic nature of the *tm5522* allele and the maternal component to its function. Overall, while the genetic analysis is somewhat complex due to the maternal requirement for *hrpk-1* activity, taken together, these genetic data support the antimorphic, weakly semi-dominant nature of the *hrpk-1(tm5522)* allele.

hrpk-1 **functionally interacts with the** ***let-7 family*** **of miRNAs.**

To test whether *hrpk-1* functions in miRNA-dependent cell fate specification, we examined potential genetic interactions between *hrpk-1* and *let-7* family of miRNAs that control temporal cell fate specification throughout larval development. The *let-7* miRNAs regulate the stage specific cell gene expression programs in a number of tissues, with the *let-7* family mutant phenotypes most evident in the *C. elegans* seam and hypodermis (for review, see [29]). Specifically, *let-7* family miRNAs, together with other heterochronic genes, regulate cell division patterns of the seam cells during larval development [30] and seam cell terminal differentiation at the transition from larval development to adulthood [31]. *mir-48, mir-241,* and *mir-84,* three members of the *let-7* miRNA family, are transcriptionally upregulated in the late L1 stage and subsequently down-regulate the expression of the *hbl-1* transcription factor during the L2 stage [30]. As a consequence of these regulatory interactions, *mir-48, mir-241,* and *mir-84* limit the proliferative seam cell division pattern of hypodermal stem cells to the L2 stage and promote subsequent L3-associated patterns of seam cell

divisions [30], (Fig 3A). *mir-48, mir-241,* and *mir-84* are genetically redundant, with single and double mutants of these microRNAs exhibiting partially penetrant cell retarded heterochronic phenotypes [30]. These phenotypes can be monitored by observing alterations in seam cell lineage as well as defects associated with a reduction in the expression of adult-specific reporters (*col-19::gfp*) after the 4th larval stage [30,32], (Fig 3B). *hrpk-1(zen17)* enhances the retarded phenotype of *mir-48 mir-241 (nDf51)* mutants (Fig 3B-D). Specifically, loss of *hrpk-1* activity enhances the retarded expression of adult hypodermal marker, *col-19::gfp(maIs105),* (Fig 3C and D) and results in an increased number of seam cells as compared to *mir-48 mir-241(nDf51)* alone (Fig 3B). This enhancement of the *mir-48 mir-241(nDf51)* heterochronic phenotype by loss of *hrpk-1* is consistent with *hrpk-1* functional requirement for efficient activity of the remaining intact *let-7* family miRNAs.

let-7, the founding member of the *let-7* family of miRNAs, controls terminal cell fate specification, which occurs during the developmental progression through the late larval stages and into the adulthood [31]. A temperature sensitive mutation that compromises but does not completely abolish let-7 activity, *let-7(n2853)*, causes a retarded development phenotype [31], [33]. *let-7(n2853)* animals have abnormal/absent alae in young adults and delayed hypodermal expression of the adult marker *col-19::gfp* at 20^{o}C (Fig 3E and F), [31]. *hrpk-1* knockout enhances retarded *col-19::gfp(maIS105)* expression (Fig 3E) and the retarded alae phenotype (Fig 3F) observed in the *let-7(n2853)* mutants. Loss of *hrpk-1* alone is not enough to induce a heterochronic phenotype (Fig 3A, D, C). The observed enhancement of the *let-7(n2853)* retarded phenotype by *hrpk-1* mutations is consistent with the hypothesis that *hrpk-1* function is important for *let-7* miRNA activity.

hrpk-1 **functionally interacts with the** ***lsy-6*** **miRNA and is required for efficient regulation of** ***lsy-6*** **target** ***cog-1*****.**

To test the hypothesis that HRPK-1 may be required for miRNA activity regulation, we looked for the effects of *hrpk-1* mutations on the activity of *lsy-6* miRNA-dependent processes. *lsy-6* regulates cell fates of two bilaterally symmetrical ASE neurons [34]. ASEL-specific expression of *lsy-6* down-regulates its key target, *cog-1*, while uninhibited *cog-1* expression within the ASER dictates that neuron's cell fate [34]. The ASEL cell fate is distinguished by the expression of a downstream reporter, *Plim-6::gfp,* an established marker for the ASEL cell fate [34], [35], (Fig 4A). Reduction of lsy-6 activity through a cis-regulatory mutation in the *lsy-6* promoter, *lsy-6(ot150),* causes a low penetrance phenotype where the ASEL neuron adopts the cell fate of ASER approximately 20% of the time [36], (Fig 4A and B). To assess *hrpk-1-lsy-6* functional interaction we removed *hrpk-1* in the presence of the reduction of function *lsy-6(ot150)* allele. Genetic mutations in *hrpk-1* significantly enhance the cell fate defective phenotype observed in the *lsy-6(ot150)* animals (Fig 4B). *hrpk-1* mutations alone are not sufficient to induce an ASEL to ASER cell fate switch (Fig 4B). Importantly, *hrpk-1* RNAi relieves the lsy-6-mediated inhibition of its target, *cog-1::gfp,* in uterine cells (Fig 4C-D), suggesting that HPRK-1 is required for efficient inhibition of *cog-1* by lsy-6 miRNA in that tissue.

hrpk-1 **functionally interacts with the** ***mir-35-42*** **family of miRNAs.**

To assess whether *hrpk-1* may be broadly required for miRNA activity, we reduced its function in other miRNA sensitized backgrounds. *mir-35-42* family of miRNAs controls fertility and embryonic development of *C. elegans* [37]. Loss of the entire *mir-35-42* miRNA family results in fully penetrant sterility and embryonic lethality phenotypes [37]. Deletion of a genomic region harboring 7 of the 8 *mir-35* family miRNAs (*mir-35-41*), *mir-35-41(nDf50),* causes animals to exhibit temperature sensitive increase in embryonic lethality and overall reduction of brood size [37], [38], (Fig 5 A and B). Combining either *hrpk-1* deletions (*hrpk-1(zen17)* and *hrpk-1(tm5522))* with the *mir-35-41(nDf50)* deletion allele results in a strong synthetic lethal phenotype where a majority of animals fail to

develop (Fig 5A). This genetic synergy in combined mutants is also recapitulated in a dramatic decrease in overall brood size (Fig 5B). In both cases, animals were reared at the semi-permissive temperature of 20ºC. *hrpk-1(tm5522)* causes a greater enhancement of the *mir-35-41(nDf50)* phenotype than *hrpk-1(zen17)* null (Fig 5 A-B), consistent with the antimorphic nature of the *hrpk-1(tm5522)* allele. Importantly, the enhancement of the *mir-35-41(nDf50)* phenotype by *hrpk-1* mutations is not simply additive, but synergistic (Fig 5A-B), consistent with the hypothesis that *hrpk-1* activity may be required for remaining *miR-42* function.

HRPK-1 is ubiquitously expressed throughout *C. elegans* development.

To gain insight into HRPK-1 function, we characterized both spatial and temporal expression of endogenous HRPK-1 using a CRISPR-generated *hrpk-1::gfp* transgene (Fig 6). *hrpk-1::gfp* is ubiquitously expressed during all *C. elegans* developmental stages (Fig 6A-D). The C-terminally tagged *hrpk-1::gfp* expression is observed in the gut, muscle, neuronal, and hypodermal tissues, where it localizes to the cell nuclei (Fig 6A, B). Interestingly, *hrpk-1::gfp* is strongly present in the animal germline, oocytes, and early embryos, where its subcellular localization is both nuclear and cytoplasmic (Fig 6B-D). The subcellular localization of HRPK-1::GFP is consistent with the predicted nuclear localization and nuclear export signals found within the *hrpk-1* sequence (Fig 1B). Our inability to detect *hrpk-1::gfp* signal in the cytoplasm of somatic cells may reflect HRPK-1 distinct functions between the soma and the germline or may simply be due to a lower expression level that falls below our detection limits. In fact, HRPK-1 somatic cytoplasmic localization has been observed large scale subcellular proteome mapping [39], suggesting that we may be limited in detecting HRPK-1 in the cytoplasm in the presence of strong nuclear expression. Overall, the spatial and temporal *hrpk-1* pattern of expression is consistent with the apparent *hrpk-1* roles in a number of developmental processes, including embryonic and larval development, as well as fertility.

Loss of *hrpk-1* modestly affect levels of select miRNAs but does not affect ALG-1/AIN-1 miRISC assembly.

Functional regulation of the miRNA activity by HRPK-1 could occur at the level of miRNA processing, miRISC assembly, or miRISC activity. To determine whether HRPK-1 is necessary for miRNA biogenesis, we cloned and sequenced miRNAs from wild type, *hrpk-1(zen17),* and *hrpk-1(tm5522)* mutant animals. We found that in general, abundance of mature miRNAs is not globally affected in *hrpk-1(zen17)* animals (Fig 7A-C, S1 Table), with only five mature miRNAs reduced 2 or more-fold in *hprk-1(zen17)* mutant and three miRNAs increased more than 2-fold (S2 Table). In contrast, *hrpk-1(tm5522)* animals have an expanded set of miRNAs reduced in abundance. Twenty-seven miRNAs, including members of the mir-35 family, were reduced 2-fold or more in the *hrpk-1(tm5522)* animals, and seven miRNAs were increased in abundance in *htpk-1(tmm5522)* mutants (S2 Table). We did observe a >2-fold decrease in lsy-6 abundance in both *hrpk-1(zen17)* and *hrpk-1(tm5522)* animals (Fig 7D and S2 Table). This reduction in lsy-6 counts could explain the functional interaction observed between *hrpk-1(-)* and *lsy-6(ot150)*. In contrast, let-7, mir-84, and mir-42 levels were not consistently decreased in *hrpk-1* mutants (Fig 7D and S1 Table). In fact, mir-84 counts were somewhat increased in both *hrpk-1(zen17)* and *hrpk-1(tm5522)* animals and let-7 and mir-42 were slightly decreased in the *hrpk-1(tm5522)* mutants only (Fig 7D and S1 Table). These data suggest that the functional interaction between *hrpk-1* mutations and *let-7(n2852), mir-48 mir-241(nDf51),* and *mir-35-41(nDf50)* miRNA mutants does not arise from a decrease in miRNA abundance of the remaining intact miRNAs (let-7, mir-84, and mir-42).

Mature miRISC formation involves Argonaute association with GW182 homologs [4]. To assess whether HRPK-1 may be needed for miRISC assembly, we tested the ability of ALG-1 to co-precipitate with its miRISC co-factor and GW182 homolog AIN-1 in *hrpk-1(zen17).* We found that

AIN-1 co-precipitates with ALG-1 in *hrpk-1* mutant animals at levels similar to those observed in wild type (Fig 7E). We did not test for ALG-2 and AIN-2 containing miRISC formation and therefore cannot rule out the possibility that HRPK-1 may be necessary for formation of miRISCs that include ALG-2 and/or AIN-2 proteins. However, we can conclude that HRPK-1 is not required for ALG-1/AIN-1 interaction as observed by our ALG-1 immunoprecipitation experiments (Fig 7E).

Discussion

HRPK-1 physically and functionally interacts with miRNA pathways.

In this manuscript we report characterizations of *hrpk-1,* which encodes an RNA binding protein HRPK-1. HRPK-1 was originally identified by MudPIT proteomics in ALG-1 co-precipitates [14], (Fig 1D). Here, we confirm that HRPK-1 can co-precipitate ALG-1 in a reciprocal experiment and show that the interaction between HRPK-1 and ALG-1 is only partially RNA-dependent (Fig1E). The relatively small amount of ALG-1 co-precipitating with HRPK-1 could reflect instability of complexes in our assay or may represent the portion of ALG-1 in complex with HRPK-1 (Fig 1E). Importantly, not only is HRPK-1 a conserved protein and an ortholog of human hnRNP K, the interaction between Argonaute and HRPK-1 also appears to be conserved as hnRNP K has previously been co-purified with three of four human AGO proteins [40].

In addition to confirming the conserved physical interaction between HRPK-1 and ALG-1, we report that *hrpk-1* is genetically required for efficient activity of several miRNAs and miRNA families: *lsy-6, let-7-family,* and *mir-35-family*. Loss of *hrpk-1* alone does not alter ASEL/ASER cell fate decisions despite enhancing the *lsy-6(ot150)* reduction-of-function phenotype. In addition to enhancing the cell fate defects observed in *lsy-6(ot150)* animals, HRPK-1 promoted lsy-6 mediated repression of lsy-6 target gene, *cog-1* (Fig 4C and D). Similarly, loss of *hrpk-1* did not cause a heterochronic phenotype normally observed in *let-7* family mutants (Fig 3), although the antimorphic

hprk-1(tm5522) allele did produce a mild alae defect (Fig 2G). Together, these data suggest that HRPK-1 is not an essential miRNA co-factor, but rather positively modulates *lsy-6* and *let-7* family miRNA activity. The synergistic genetic interaction between *hrpk-1* mutations and *mir-35-41(nDf50)* is also consistent with a hypothesized role for *hrpk-1* as a positive co-factor of mir-42 activity. Overall, we show that HRPK-1 physically interacts ALG-1, a major component of miRLC/miRISC and functionally interacts with several miRNAs in a number of developmental processes.

hrpk-1 **subcellular localization**

Overall, the ubiquitous expression of *hrpk-1* is consistent with its pleotropic effects on *C. elegans* development. We observed a strong nuclear expression of endogenous *hrpk-1* (Fig 6) and both nuclear and cytoplasmic HRPK-1::GFP localization in the germline, oocytes, and early embryos. This is not surprising as HRPK-1 does contain a predicted nuclear localization signal and a predicted nuclear export signal (Fig 1B). Despite our inability to definitively detect HRPK-1::GFP in the cytoplasm of somatic tissues, a recent report mapping the subcellular-specific proteomes in a number of *C. elegans* tissues places HRPK-1 in the hypodermal cytoplasm in addition to the nucleus using a proximity ligation dependent assay [39]. This assay may be able to capture transient protein shuttling and likely has a higher sensitivity than our fluorescent reporter observations. We would argue that the observed steady-state nuclear HRPK-1::GFP localization does not mean there is no function for HRPK-1 in the cytoplasm. In fact, given the biochemical interaction between ALG-1 and HRPK-1, we hypothesize that cytoplasmic HRPK-1 activity may in fact be required for its functional interaction with the miRNA pathways. It remains to be seen whether nuclear HRPK-1 localization or movement between the nucleus and the cytoplasm plays a role in miRNA-dependent gene expression regulation.

How might HRPK-1 enhance miRNA gene repressive activity?

Overall, several molecular models can explain the genetic and physical interactions between HRPK-1 and miRNA machinery. It is possible that HRPK-1 may interact with ALG-1 at the miRNA Loading Complex (miRLC) and participate in mature miRNA biogenesis (Fig 8A). We observed miRNA abundance changes for a small subset of miRNAs, including lsy-6, in *hrpk-1* mutant animals (Fig 7A-D and S2 Table). The observed functional interaction between *hrpk-1* and *lsy-6* mutations could therefore be explained by a reduced abundance of lsy-6 miRNA, potentially placing HRPK-1 in the *lsy-6* processing pathway. However, the abundances of the majority of miRNAs, including the *let-7-family* and *mir-42* were not consistently decreased between wild type and *hprk-1* mutants (S1 Table and Fig 7A-D). This observation suggests that the functional interaction between *hrpk-1* mutants and *let-7(n2853), mir-48 mir-241(nDf51),* and *mir-35-41(nDf50)* (Figs 3 and 5) is likely not due to *hrpk-1(-)* effects on miRNA processing. In fact, most mature miRNA abundances are not affected in *hrpk-1(zen17)* animals (Fig 7A-C, S1 Table). HRPK-1 involvement at the level of miRLC may therefore be limited to a small subset of miRNAs, including lsy-6. However, we cannot at this point rule out the possibility that HRPK-1 may play a broader role in miRLC formation or miRNA processing. The greater reduction of miRNA numbers in *hrpk-1(tm5522)* compared to *hrpk-1(zen17)* mutants hints at a possible explanation for the more severe phenotypes observed in *hrpk-1(tm5522)* animals, potentially through sequestration of components essential for miRNA processing or stability. Further work will be needed to characterize the extent to which HRPK-1 may be involved in miRNA processing and/or stability and the cause of the antimorphic nature of the *hrpk-1(tm5522)* allele.

We found that HRPK-1 is not required for ALG-1/AIN-1 miRISC assembly, as *hrpk-1(zen17)* animals have an intact ALG-1/AIN-1 miRISC (Fig 7E). This observation is consistent with the hypothesis that HRPK-1 may interact with ALG-1 downstream of miRISC formation, possibly via the target mRNAs. We favor this hypothesis, as it is difficult to imagine a sole role for HRPK-1 at the level

of miRLC that does not globally affect mature miRNA biogenesis or mature miRISC formation. Interestingly, the interaction between HRPK-1 and ALG-1 is only partially RNA-dependent (Fig 1E), suggesting that RNA is not necessary for this interaction to occur but may enhance it. HRPK-1 is a member of the KH domain family of proteins, which are known to be RNA binding proteins with diverse functions. These functions could include roles in mRNA processing, mRNA stability and folding, and mRNA transport out of the nucleus, and translational control. It is possible that, similar to other hnRNP proteins, HRPK-1 has diverse functions and may coordinate with miRNA pathways on multiple levels, perhaps even by bridging the miRLC with miRISC. In addition to a potential role in miRNA processing for subset of miRNAs (Fig 8A), HRPK-1 may stimulate miRNA/miRISC activity by increasing miRNA target site availability through mRNA folding (Fig 8B). In this model, HRPK-1 association with target mRNAs and miRISC may enhance miRISC accessibility and binding to target mRNAs and therefore increase the target gene repression (Fig 8B). In addition, HRPK-1 could stimulate the interaction between miRISC and downstream effector complexes (Fig 8C). Identification of HRPK-1 RNA binding sites and their proximity to miRNA target sites will in the future help characterize the physical relationship between the two.

Given the diversity of hnRNP and KH domain proteins functions, we must allow for the possibility that multiple, miRISC-dependent and independent HRPK-1 activity synergizes with the miRNA-mediated target regulation. For example, an HRPK-1 role in mRNA processing could increase miRNA site availability. Identifying the impacts of HRPK-1 loss on alternative splicing of mRNAs and the resulting changes in miRNA binding site availability can in the future shed light on the plausibility of this model. It should be noted that none of the proposed models are mutually exclusive and multiple HRPK-1 functions could synergize, directly and/or indirectly, with the miRNA gene regulatory pathways. We look forward to further investigating the mechanisms through which HRPK-1 and miRNAs cooperate to facilitate gene repression.

Overall, our results demonstrate that HRPK-1, a KH domain RNA binding protein, physically and functionally interacts with miRNA-mediated gene repression. Other KH domain RNA binding proteins have been shown to biochemically and genetically interact with the miRNA machinery. These include the *C. elegans* translational repressor, a Quaking homolog, and a KH domain protein, GLD-1, among others [28], [41] and VGLN-1 [24]. Additional KH-domain proteins and other hnRNPs have been detected in large-scale mass spectrometry experiments [41], [14], [42]. The molecular mechanisms by which RNA binding proteins synergize with miRNA pathways to regulate mRNA expression are diverse and remain largely unknown. Further studies to understand the mechanism of functional interactions between RBPs, including HRPK-1, and miRNA-mediated gene repression will shed light on how these two classes of post-transcriptional gene regulators cooperate to regulate animal development.

Materials and methods

Strain maintenance, RNAi, and phenotypic assessments

C. elegans strains were grown in standard conditions on NGM plates using OP50 as a food source [43]. Strains were maintained at 20ºC unless otherwise noted. RNAi gene knockdown was performed as previously described [44]. Briefly, PS3662 or OH7310 animals were placed on *hrpk-1* RNAi food and the F1 progeny were scored for the *cog-1::gfp* presence in vulval and uterine cells.

For the *mir-48 mir-241(nDf51)* assay, young adults were scored for seam and hypodermal *col-19::gfp* expression, alae formation, and seam cell number. Seam cells numbers were obtained by counting the seam cells located between the pharynx and the anus of a given animal. Phenotypes were scored on either the Zeiss Axioplan 2 or the Leica DM6 upright microscopes equipped with DIC and epifluorescence. For *mir-35-41(nDf50)* assay, animals were scored for sterility, brood size and embryonic lethality. Animal sterility, embryonic lethality, and brood size were assessed by scoring

entire broods of individual animals. Animals were considered sterile if they were unable to produce any progeny, dead or alive. Brood size refers to the total number of progeny produced, including dead embryos. Percent embryonic lethality was calculated as follows: # of dead embryos/total progeny (live progeny + dead embryos). Vulval bursting was visually assessed beginning at the Day 1 young adult stage and daily thereafter.

CRISPR-based genome editing

hrpk-1(zen15) and *hrpk-1(zen-17)* deletion alleles were produced using CRISPR/Cas9 genome editing using *hrpk-1* site specific guides 1 and 9, corresponding to the 5' and 3' ends of the gene, respectively. The following *hrpk-1* guides were used to generate the deletions: *hrpk-1* guide 1, ACTGTCTGTTCCATTAATAG and *hrpk-1* guide 9, CAAGGCCGTGAACGATTCGG. *hrpk-1(zen17)* was outcrossed seven times and *hrpk-1(zen15)* was outcrossed twice. The entire *hrpk-1* locus was sequenced to confirm the nature of the deletion in each mutant.

Endogenously tagged *hrpk-1::gfp* strains were generated by inserting a worm codon-optimized GFP coding sequence and a self-excising cassette (SEC) into the C-terminus of endogenous *hrpk-1* locus just before the stop codon through CRISPR/Cas-9 triggered homologous recombination [45]. The SEC was then excised as described [45]. The donor sequence was generated by subcloning 596 bp upstream of the *hrpk-1* stop codon and 600 bp downstream of *hrpk-1* stop codon into the pDD282 vector [45] using Hi Fi assembly kit (NEB). The *hrpk-1* stop codon was eliminated from the donor sequence to allow in frame GFP tag addition. A PAM site mutation corresponding to guide 9 was included in the donor DNA sequence resulting in the sequence change of [CAAGGCCGTGAACGATTCGGTGG] change to [CAAGGCCGTGAACGATTCGGTCG] immediately upstream of the GFP tag sequence. Animal microinjections were performed as previously described [46]. Six independent *hrpk-1::gfp* lines were obtained and the resulting endogenously tagged *hrpk-*

1::gfp loci was sequenced. Since all six lines looked superficially wild type and showed the same *hrpk-1::gfp* expression pattern, a single line was chosen for an in-depth analysis. The *hrpk-1::gfp(zen64)* strain was outcrossed twice and assessed for *hrpk-1* functional integrity. *hrpk-1::gfp* transgenic line had wild type fertility and embryonic viability (S3 Fig), confirming that the GFP-tagged HRPK-1 retained its wild type activity.

The following primers were used in generation of the *hrpk-1* donor sequence in order to place the GFP sequence at the C-terminus of *hrpk-1*:

5' homology arm forward primer:	5' - CGACGGCCAGTCGCCGGCAGATCGTATGGAGGAGCTATTAC - 3'
5' homology arm reverse primer:	5' - CCTGAGGCTCCCGATGCTCCGACAGATGCACCGAATCGTTC - 3'
3' homology arm forward primer:	5' – GGATGACGATGACAAGAGATAAGTTCTGGTGTTCGTACTCTTC -3'
3' homology arm reverse primer:	5' – GACCATGTTATCGATTTCCGCCCTTAGGAGATAATTTGC – 3'

Extract preparation and immunoprecipitation (IP)

Worm extracts were prepared as previously described [47] with the following modifications. Mixed stage animals were homogenized using a Bullet blender (MIDSCI). Briefly, 300μL worm pellets were mixed with RNAse free Rhino beads (MIDSCI) and 300μL lysis buffer and homogenized at the highest setting for 4 minutes. Homogenate was then moved to a fresh tube and spun at 13,000xg for 20 minutes to clarify the extract. The extracts were then used for immunoprecipitation experiments or were flash frozen in liquid nitrogen and stored at -80^{o}C.

ALG-1 immunoprecipitation and Western blotting were performed as previously described [48] using Protein A Dynabeads (ThermoFisher). HRPK-1 detection was done using a custom rabbit anti-HRPK-1 antibody (Pocono) generated against the C-terminal peptide of HRPK-1 (CVRNSTQGRERFGGSV) at the 1:1000 dilution. HRPK-1 immunoprecipitation was performed using the same method as ALG-1 immunoprecipitation [48], with the anti-HRPK-1 antibody covalently crosslinked to the Protein A Dynabeads (ThermoFisher) using dimethylpimelimidate1. Mouse anti-tubulin antibody (Sigma-Aldrich) was used to detect tubulin as a loading control.

RNA preparation and small RNA sequencing

RNA from mixed stage animals was prepared as previously described [47] with the following modifications. Mixed stages animals resuspended in 250μL water were mixed with 1ml of Trizol (Fisher Scientific) and RNAse free Rhino beads (MIDSCI) and homogenized using a Bullet blender (MIDSCI) at the highest setting for 4 minutes. Homogenate was then moved into a fresh tube, mixed with 212μL of chloroform, and spun down to separate the phases. All remaining steps of the RNA purification were performed as previously described [47].

For small RNA libraries preparation, small RNAs were first size selected by gel purification as described in [49]. The size selected RNA was then used to construct small RNA libraries using the NEXTflex Small RNA Library Prep kit v3 (Bioo Scientific) and sequenced on the Illumina HighSeq instrument at the Kansas University Genome Sequencing Core. Data analysis was performed as previously described [14]. The total mapped reads across two replicates were as follows: N2 (7,386,035), UY38 (7,679,177), and UY42 (7,540,761).

Microscopy and statistics

Localization of the endogenously tagged HRPK-1::GFP transgene was imaged using Zeiss Axioplan 2 upright microscope equipped with a Zeiss Axiocam HR digital camera. Images were assembled using Photoshop. Contrast and brightness of images were not adjusted. F-test was used to analyze brood size, t-test was used to analyze embryonic lethality, and chi-square was used to analyze all other phenotypic data.

Strains used in this study

N2 wild type

UY44 hrpk-1(zen15)

UY38 hrpk-1(zen17)

UY39 hrpk-1(zen17); maIs105[col-19::gfp]

UY42 hrpk-1(tm5522)

UY43 hrpk-1(tm5522); maIs105[col-19::gfp]

OH3646 otIs114[Plim-6::gfp + rol-6(su1006)] ; lsy-6(ot150)

UY46 hrpk-1(zen17) otIs114[Plim-6::gfp + rol-6(su1006)]; lsy-6(ot150)

UY54 hrpk-1(zen17) otIs114[Plim-6::gfp + rol-6(su1006)]

UY9 hrpk-1(tm5522) otIs114[Plim-6::gfp + rol-6(su1006)]; lsy-6 (ot150)

UY18 hrpk-1(tm5522) otIs114[Plim-6::gfp + rol-6(su1006)]

PS3662 syIs63[cog-1::gfp + unc-119(+)]

OH7310 otIs193 [cog-1p::lsy-6hp + rol-6(su1006)] syIS63[cog-1::gfp + unc-119(+)]

MT14119 mir-35-41(nDf50)

UY56 hrpk-1(zen17)/ht2gfp; mir-35-41(nDf50)

UY55 hrpk-1(tm5522)/ht2gfp; mir-35-41(nDf50)

VT1296 mir-241,mir-48(nDf51) maIs105[col19::GFP]

UY67 hrpk-1(zen17); mir-241 mir-48(nDf51) maIs105[col19::gfp]

UY68 hrpk-1(tm5522); mir-241 mir-48(nDf51) maIs105[col19::gfp]

HML11 maIs105[col19::gfp] lin-2 (e1309) let-7 (n2853)

UY157 hrpk-1(zen17); maIs105[col19::gfp] lin-2 (e1309) let-7 (n2853)

VT3841 alg-1(tm492)

UY66 hrpk-1::gfp(zen64)

Acknowledgements

We are grateful to the Caenorhabditis Genetics Center (CGC), funded by NIH Office of Research Infrastructure Programs (P40 OD010440), which provided some of the strains used in this project. We thank the National BioResource Project (NBRP) at the Tokyo Women's Medical University School of Medicine for providing the *hrpk-1(tm5522)* allele described in this study. We thank Yin Wang for technical support. We are grateful to the Ambros lab, where the HRPK-1 interaction with ALG-1 was initially discovered. We thank C. Hammell for strains and the critical reading of this manuscript, and M. Han for AIN-1 antisera. This work has been supported by Kansas INBRE, P20GM103418 to L.L. and A.Y.Z., and R35GM124828 to A.Y.Z.

References

1. Rajman M, Schratt G. MicroRNAs in neural development: from master regulators to fine-tuners. Development. Oxford University Press for The Company of Biologists Limited; 2017 Jul 1;144(13):2310–22.

2. Ivey KN, Srivastava D. microRNAs as Developmental Regulators. Cold Spring Harb Perspect Biol. Cold Spring Harbor Lab; 2015 Jul 1;7(7):a008144.

3. Bartel DP. Metazoan MicroRNAs. Cell. 2018 Mar 22;173(1):20–51.

4. Jonas S, Izaurralde E. Towards a molecular understanding of microRNA-mediated gene silencing. Nature Publishing Group. Nature Publishing Group; 2015 Jul;16(7):421–33.

5. Treiber T, Treiber N, Plessmann U, Harlander S, Daiß J-L, Eichner N, et al. A Compendium of RNA-Binding Proteins that Regulate MicroRNA Biogenesis. Molecular Cell. 2017 Apr 20;66(2):270–284.e13.

6. Schopp IM, Amaya Ramirez CC, Debeljak J, Kreibich E, Skribbe M, Wild K, et al. Split-BioID a conditional proteomics approach to monitor the composition of spatiotemporally defined protein complexes. Nat Comms. Nature Publishing Group; 2017 Jun 6;8:15690.

7. Hammell CM, Lubin I, Boag PR, Blackwell TK, Ambros V. nhl-2 Modulates microRNA activity in Caenorhabditis elegans. Cell. 2009 Mar 6;136(5):926–38.

8. HOck J, Weinmann L, Ender C, Rüdel S, Kremmer E, Raabe M, et al. Proteomic and functional analysis of Argonaute-containing mRNA-protein complexes in human cells. EMBO Rep. EMBO Press; 2007 Nov;8(11):1052–60.

9. Alessi AF, Khivansara V, Han T, Freeberg MA, Moresco JJ, Tu PG, et al. Casein kinase II promotes target silencing by miRISC through direct phosphorylation of the DEAD-box RNA helicase CGH-1. Proc Natl Acad Sci USA. National Academy of Sciences; 2015 Dec 29;112(52):E7213–22.

10. Parry DH, Xu J, Ruvkun G. A Whole-Genome RNAi Screen for C. elegans miRNA Pathway Genes. Current Biology. 2007 Dec;17(23):2013–22.

11. Nolde MJ, Saka N, Reinert KL, Slack FJ. The Caenorhabditis elegans pumilio homolog, puf-9, is required for the 3'UTR-mediated repression of the let-7 microRNA target gene, hbl-1. Dev Biol. 2007 May 15;305(2):551–63.

12. Ding XC, Slack FJ, Großhans H. The let-7 microRNA interfaces extensively with the translation machinery to regulate cell differentiation. Cell Cycle. 2008 Oct;7(19):3083–90.

13. Rausch M, Ecsedi M, Bartake H, Müllner A, Großhans H. A genetic interactome of the let-7 microRNA in C. elegans. Dev Biol. 2015 May 15;401(2):276–86.

14. Zinovyeva AY, Veksler-Lublinsky I, Vashisht AA, Wohlschlegel JA, Ambros VR. Caenorhabditis elegans ALG-1 antimorphic mutations uncover functions for Argonaute in microRNA guide strand selection and passenger strand disposal. Proc Natl Acad Sci USA. 2015 Sep 22;112(38):E5271–80.

15. Geuens T, Bouhy D, Timmerman V. The hnRNP family: insights into their role in health and disease. Hum Genet. Springer Berlin Heidelberg; 2016 Aug;135(8):851–67.

16. Dreyfuss G, Kim VN, Kataoka N. Messenger-RNA-binding proteins and the messages they carry. Nat Rev Mol Cell Biol. Nature Publishing Group; 2002 Mar;3(3):195–205.

17. Kooshapur H, Choudhury NR, Simon B, Mühlbauer M, Jussupow A, Fernandez N, et al. Structural basis for terminal loop recognition and stimulation of pri-miRNA-18a processing by hnRNP A1. Nat Comms. Nature Publishing Group; 2018 Jun 26;9(1):2479.

18. Svitkin YV, Yanagiya A, Karetnikov AE, Alain T, Fabian MR, Khoutorsky A, et al. Control of translation and miRNA-dependent repression by a novel poly(A) binding protein, hnRNP-Q. Lykke-Andersen J, editor. PLoS Biol. Public Library of Science; 2013;11(5):e1001564.

19. Siomi H, Matunis MJ, Michael WM, Dreyfuss G. The pre-mRNA binding K protein contains a novel evolutionarily conserved motif. Nucleic Acids Research. Oxford University Press; 1993 Mar 11;21(5):1193–8.

20. Valverde R, Edwards L, Regan L. Structure and function of KH domains. FEBS J. Blackwell Publishing Ltd; 2008 Jun;275(11):2712–26.

21. Musco G, Stier G, Joseph C, Castiglione Morelli MA, Nilges M, Gibson TJ, et al. Three-dimensional structure and stability of the KH domain: molecular insights into the fragile X syndrome. Cell. 1996 Apr 19;85(2):237–45.

22. Kruse C, Willkomm D, Gebken J, Schuh A, Stossberg H, Vollbrandt T, et al. The multi-KH protein vigilin associates with free and membrane-bound ribosomes. Cell Mol Life Sci. Birkhäuser-Verlag; 2003 Oct;60(10):2219–27.

23. García-Mayoral MF, Hollingworth D, Masino L, Díaz-Moreno I, Kelly G, Gherzi R, et al. The structure of the C-terminal KH domains of KSRP reveals a noncanonical motif important for mRNA degradation. Structure. 2007 Apr;15(4):485–98.

24. Zabinsky RA, Weum BM, Cui M, Han M. RNA Binding Protein Vigilin Collaborates with miRNAs To Regulate Gene Expression for Caenorhabditis elegans Larval Development. G3: GenesIGenomesIGenetics. G3: Genes, Genomes, Genetics; 2017 Aug 7;7(8):2511–8.

25. Shin CH, Lee H, Kim HR, Choi KH, Joung J-G, Kim HH. Regulation of PLK1 through competition between hnRNPK, miR-149-3p and miR-193b-5p. Cell Death Differ. Nature Publishing Group; 2017 Nov;24(11):1861–71.

26. Fan B, Sutandy FXR, Syu G-D, Middleton S, Yi G, Lu K-Y, et al. Heterogeneous Ribonucleoprotein K (hnRNP K) Binds miR-122, a Mature Liver-Specific MicroRNA Required for Hepatitis C Virus Replication. Molecular & Cellular Proteomics. American Society for Biochemistry and Molecular Biology; 2015 Nov;14(11):2878–86.

27. Fan B, Lu K-Y, Reymond Sutandy FX, Chen Y-W, Konan K, Zhu H, et al. A human proteome microarray identifies that the heterogeneous nuclear ribonucleoprotein K (hnRNP K) recognizes the 5' terminal sequence of the hepatitis C virus RNA. Molecular & Cellular Proteomics. 2014 Jan;13(1):84–92.

28. Akay A, Craig A, Lehrbach N, Larance M, Pourkarimi E, Wright JE, et al. RNA-binding protein GLD-1/quaking genetically interacts with the mir-35 and the let-7 miRNA pathways in Caenorhabditis elegans. Open Biology. Royal Society Journals; 2013 Nov 1;3(11):130151.

29. Ambros V, Ruvkun G. Recent Molecular Genetic Explorations of Caenorhabditis elegans MicroRNAs. Genetics. 2018 Jul;209(3):651–73.

30. Abbott AL, Alvarez-Saavedra E, Miska EA, Lau NC, Bartel DP, Horvitz HR, et al. The let-7 MicroRNA Family Members mir-48, mir-84, and mir-241 Function Together to Regulate Developmental Timing in Caenorhabditis elegans. Developmental Cell. 2005 Sep;9(3):403–14.

31. Reinhart BJ, Slack FJ, Basson M, Pasquinelli AE, Bettinger JC, Rougvie AE, et al. The 21-nucleotide let-7 RNA regulates developmental timing in Caenorhabditis elegans. Nature. 2000 Feb 24;403(6772):901–6.

32. Abrahante JE, Miller EA, Rougvie AE. Identification of heterochronic mutants in Caenorhabditis elegans: temporal misexpression of a collagen:: green fluorescent protein fusion gene. Genetics. Genetics Soc America; 1998;149(3):1335–51.

33. Vella MC, Choi E-Y, Lin S-Y, Reinert K, Slack FJ. The C. elegans microRNA let-7 binds to imperfect let-7 complementary sites from the lin-41 3'UTR. Genes & Development. Cold Spring Harbor Lab; 2004 Jan 15;18(2):132–7.

34. Johnston RJ, Hobert O. A microRNA controlling left/right neuronal asymmetry in Caenorhabditis elegans. Nature. 2003 Dec 18;426(6968):845–9.

35. Chang SS, Johnston RJR, Hobert OO. A transcriptional regulatory cascade that controls left/right asymmetry in chemosensory neurons of C. elegans. Genes & Development. 2003 Sep 1;17(17):2123–37.

36. Sarin S, O'Meara MM, Flowers EB, Antonio C, Poole RJ, Didiano D, et al. Genetic Screens for Caenorhabditis elegans Mutants Defective in Left/Right Asymmetric Neuronal Fate Specification. Genetics. 2007 Aug 1;176(4):2109–30.

37. Alvarez-Saavedra E, Horvitz HR. Many families of C. elegans microRNAs are not essential for development or viability. Curr Biol. 2010 Feb 23;20(4):367–73.

38. McJunkin K, Ambros V. The embryonic mir-35 family of microRNAs promotes multiple aspects of fecundity in Caenorhabditis elegans. G3: GeneslGenomeslGenetics. 2014 Sep;4(9):1747–54.

39. Reinke AW, Mak R, Troemel ER, Bennett EJ. In vivo mapping of tissue- and subcellular-specific proteomes in Caenorhabditis elegans. Sci Adv. 2017 May;3(5):e1602426.

40. Landthaler M, Gaidatzis D, Rothballer A, Chen PY, Soll SJ, Dinic L, et al. Molecular characterization of human Argonaute-containing ribonucleoprotein complexes and their bound target mRNAs. RNA. Cold Spring Harbor Lab; 2008 Dec;14(12):2580–96.

41. Dallaire A, Frédérick P-M, Simard MJ. Somatic and Germline MicroRNAs Form Distinct Silencing Complexes to Regulate Their Target mRNAs Differently. Developmental Cell. 2018 Oct 22;47(2):239–247.e4.

42. Landthaler M, Gaidatzis D, Rothballer A, Chen PY, Soll SJ, Dinic L, et al. Molecular characterization of human Argonaute-containing ribonucleoprotein complexes and their bound target mRNAs. RNA. 2008 Dec;14(12):2580–96.

43. Brenner S. The Genetics of CAENORHABDITIS ELEGANS. Genetics. 1974 May 7;77:71–94.

44. Kamath RS, Fraser AG, Dong Y, Poulin G, Durbin R, Gotta M, et al. Systematic functional analysis of the Caenorhabditis elegans genome using RNAi. Nature. 2003 Jan 16;421(6920):231–7.

45. Dickinson DJ, Pani AM, Heppert JK, Higgins CD, Goldstein B. Streamlined Genome Engineering with a Self-Excising Drug Selection Cassette. Genetics. Genetics; 2015 Aug;200(4):1035–49.

46. Mello CC, Kramer JM, Stinchcomb D, Ambros V. Efficient gene transfer in C.elegans: extrachromosomal maintenance and integration of transforming sequences. EMBO J. European Molecular Biology Organization; 1991 Dec;10(12):3959–70.

47. Zinovyeva AY, Bouasker S, Simard MJ, Hammell CM, Ambros V. Mutations in conserved residues of the C. elegans microRNA Argonaute ALG-1 identify separable functions in ALG-1 miRISC loading and target repression. Public Library of Science; 2014 Apr;10(4):e1004286.

48. Zou Y, Chiu H, Zinovyeva A, Ambros V, Chuang C-F, Chang C. Developmental decline in neuronal regeneration by the progressive change of two intrinsic timers. Science. 2013 Apr 19;340(6130):372–6.

49. Gu W, Claycomb J, Batista P, Mello C, Conte D. Cloning Argonaute-Associated Small RNAs from Caenorhabditis elegans. In: Hobman TC, Duchaine TF, editors. Methods in Molecular Biology. Humana Press; 2011. pp. 251–280–280.

Figure legends

Fig 1. Multiple *hrpk-1* alleles produce deletions within the *hrpk-1* locus; ALG-1 co-precipitates with HRPK-1. (**A**) A schematic showing the predicted exon/intron structure of *hrpk-1* gene. *hrpk-1* alleles *tm5522, zen17,* and *zen15* delete parts or all of *hrpk-1*. (**B**) The *hrpk-1(tm5522)* allele is predicted to produce a truncated form of HRPK-1 protein, removing half of the first KH domain, second KH domain, and part of the PLD domain. NLS—predicted nuclear localization signal, KH—KH domain, NES—predicted nuclear export signal, PLD—prion like domain. (**C**) Western blotting for HRPK-1 protein detects the HRPK-1(tm5522) truncated protein at ~27kDA (highlighted by *). No protein is detected from the *hrpk-1(zen17)* and *hrpk-1(zen15)* null animals. Tubulin is detected as a loading control. (**D**) HRPK-1 was identified by MudPIT mass spectrometry in ALG-1 co-precipitates [14]. NSAF = normalized spectral abundance factor. (**E**) Western blotting for HRPK-1 and ALG-1 proteins in the HRPK-1 immunoprecipitates treated and untreated with RNAse A. Tubulin is detected as a loading control for input. Input = 10% of IP. **this non-specific band is most likely antibody heavy chain.

Fig 2. *hrpk-1* mutations cause developmental defects at 20ºC and 25ºC. *hrpk-1(zen17)* and *hrpk-1(tm5522)* mutations result in temperature sensitive animal sterility (**A**), embryonic lethality (**B**), and reduced brood size (**C**). *hrpk-1(zen17)* and *hrpk-1(tm5522)* mutations cause abnormal gonad formation (**D**, quantified in **E**), vulval bursting in day 3 or older adults (**F**), and defects in young adult alae formation (**G**). Bar in (**D**)=50μm. *$p \leq 0.05$, **$p \leq 0.01$, ***$p \leq 0.001$.

Fig 3. *hprk-1* functionally interacts with the *let-7* family of miRNAs. (**A**) Schematic seam cell lineages of wild type and *mir-241 mir-48* mutant animals throughout larval development. (**B**) *hrpk-1*

mutations increase the seam cell numbers in *mir-48 mir-241(nDf51)* young adults. (**C**) Loss of wild type *hrpk-1* activity enhances the retarded hypodermal *col-19::gfp* expression phenotype of *mir-48 mir-241(nDf51)* mutants (quantified in (**D**)). *hrpk-1(zen17)* enhances the retarded (**E**) alae formation phenotype and (**F**) *col-19::gfp* expression observed in *let-7(n2853)* animals at 20ºC. Animals scored in (**B**-**E**) carry the *col-19::gfp(maIS105)* transgene. All animals in (**E, F**) carry *lin-2(e1309),* which suppresses the vulval bursting of *let-7(n2853)* animals through a non-heterochronic mechanism. Bar in (**C**)=100*μ*m. **p≤0.05, **p≤0.01, *** p≤0.001, **** p≤0.0001.*

Fig 4. *hrpk-1* function is required for efficient *lsy-6* miRNA activity. *Plim-6::gfp* reporter marks the ASEL cell fate (**A**). The low penetrance defective cell fate phenotype observed in *lsy-6(ot150)* animals is enhanced by *hrpk-1* mutations (**B**). (**C**) *hrpk-1* RNAi relieves the lsy-6-mediated repression of *cog-1::gfp* in the uterine cells, quantified in (**D**). Animals in (B) also carry *Plim-6::gfp* reporter. Bar in (C)=20*μ*m. ****p<0.001.*

Fig 5. ***hrpk-1* mutations enhance *mir-35-41(nDf51)* mutant phenotype at 20ºC**. *hprk-1* mutations enhance *mir-35-41(nDf51)* embryonic lethality (**A**) and further reduces *mir-35-41(nDf51)* brood sizes (**B-C**). (**C**) shows the brood breakdown by live and dead progeny. **p<0.05* and ****p<0.001.*

Fig 6. **Endogenously tagged *hrpk-1::gfp* transgene *(hrpk-1(zen64))* is expressed throughout *C. elegans* development.** (**A**) L1 larva shows ubiquitous HRPK-1::GFP expression in the nuclei of somatic tissues and the germline precursor cells. (**B**) HRPK-1::GFP fluorescence in an adult animal highlights ubiquitous HRPK-1 expression in somatic tissues and in the animal's germline. Zoom in micrographs of (**B**) highlight strong nuclear and cytoplasmic expression in the germline (**C**) and early embryos (**D**). Bar in (**A**), (**C**), (**D**)=20*μ*m, bar in (**B**)=100*μ*m.

Fig 7. **miRNA abundances and miRISC formation in *hrpk-1* mutant animals**. Mature miRNA abundance in wild type and *hrpk-1* mutant animals (**A-C**). The black line represents a perfect 1:1 correlation between wild type and *hrpk-1* mutant miRNA abundances. Grey lines delineate a 2-fold difference in abundance. (**B**) Zoom in of grey box in (**A**). (**C**) Zoom in of the grey box in (**B**). Both miRNA and miRNA* abundances are graphed. (**D**) Average miRNA abundances for miRNAs whose function is affected by *hrpk-1* mutations in our functional assays. (**E**) AIN-1 co-precipitates with ALG-1 in *hrpk-1* mutant animals to levels similar to wild type.

Fig 8. **Models representing potential mechanisms through which HRPK-1 synergizes with the miRISC on mRNA targets**. These models are not mutually exclusive. (**A**) HRPK-1 may cooperate with miRLC and assist in miRNA processing. (**B**) HRPK-1 may enhance miRISC activity by increasing miRNA target site availability through mRNA folding and enhancing miRISC::RNA binding. (**C**) HRPK-1 may bind mRNAs at sites near miRNA target sites and enhance miRISC::mRNA target interaction through miRISC binding. In this model, HRPK-1 may also increase miRISC activity through augmenting miRISC interaction with downstream effector complexes.

S1 Fig. *hrpk-1(zen17)* and *hrpk-1(zen15)* show similar phenotypes. *hrkp-1(zen15)* and *hrpk-1(zen17)* produce similar levels of sterility (**A**), embryonic lethality (**B**), and brood size (**C**). An increase in embryonic lethality in *hrpk-1(zen15)* mutant animals (**D**) is most likely due the difference in the number of outcrosses between the strains, with *hrpk-1(zen17)* being outcrossed seven times, while *hrpk-1(zen15)* was outcrossed only twice. ****p≤0.001*

S2 Fig. ***hrpk-1(tm5522)* is weakly semi-dominant and *hrpk-1* is required maternally.** Genetic analyses of *hrpk-1(zen17)* and *hrpk-1(tm5522)* alleles reveal that *hrpk-1* activity has a maternal component for some developmental processes such as fertility (**A**), brood size (**B**), and embryonic viability (**C**), but not for vulval integrity in day 3 or older adults (**D**). *hrpk-1(tm5522)* appears to be weakly semi-dominant as evidenced by the presence of defects observed in *hrpk-1(tm5522)/+* and *hrpk-1(tm5522)/hrpk-1(zen17)* animals (**A-D**). Genotype of the score animals is shown. m- indicates that scored animals came from homozygous mutant mothers, m+ indicates that scored animals were progeny of wild type mothers. *hrpk-1(tm5522)m/hrpk-1(zen17)p* animals came from a cross between *hrpk-1(tm5522)* mothers and *hrpk-1(zen17)* fathers. *hrpk-1(tm5522)p/hrpk-1(zen17)m* animals came from *hrpk-1(zen17)* mothers and *hrpk-1(tm5522)* fathers.

S3 Fig. GFP-tagged endogenous HRPK-1 retains its activity. C-terminal HRPK-1 GFP tag does not affect animal fertility (**A**) or embryonic viability (**B**).

Figure 1

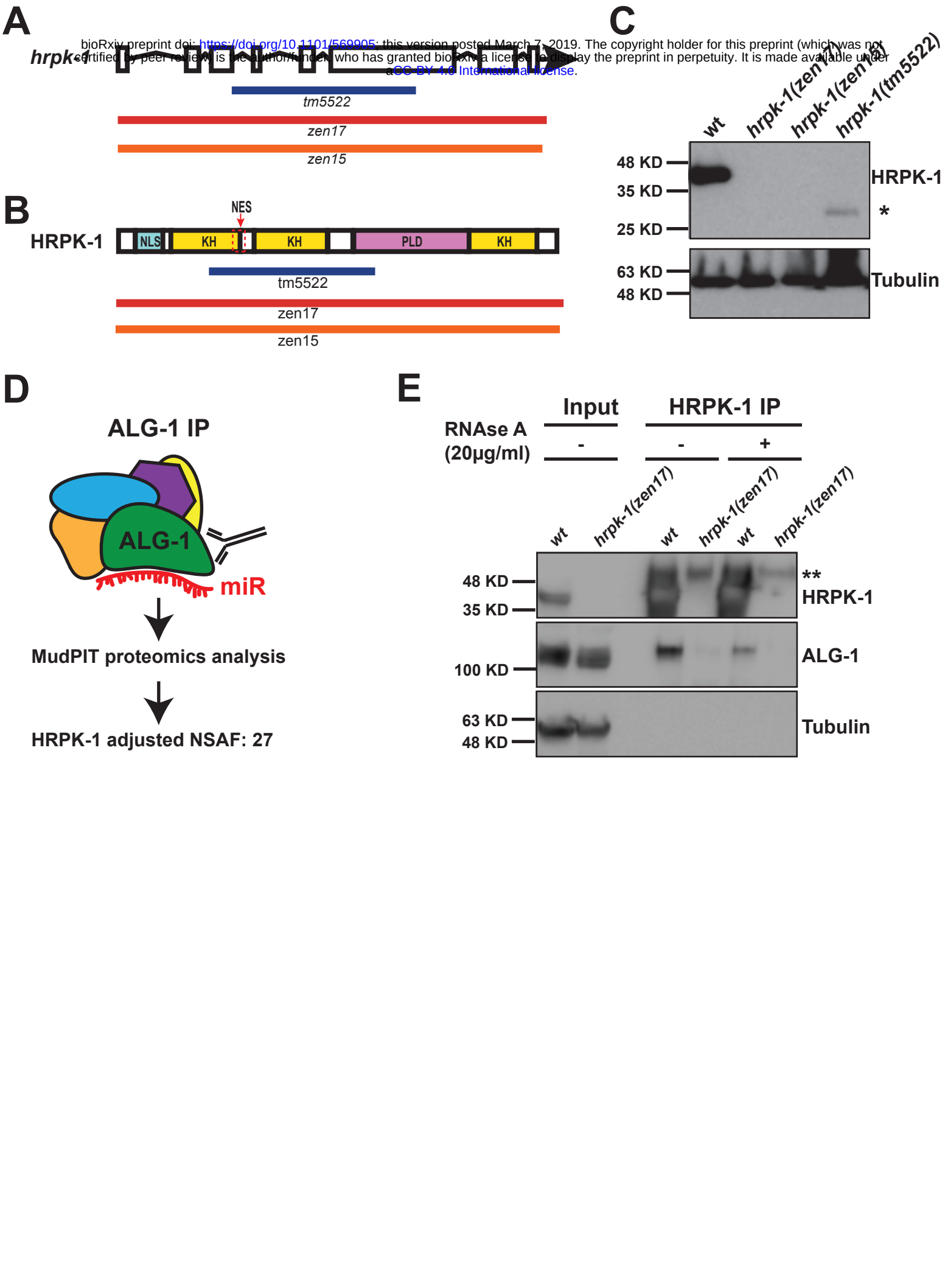

Figure 2

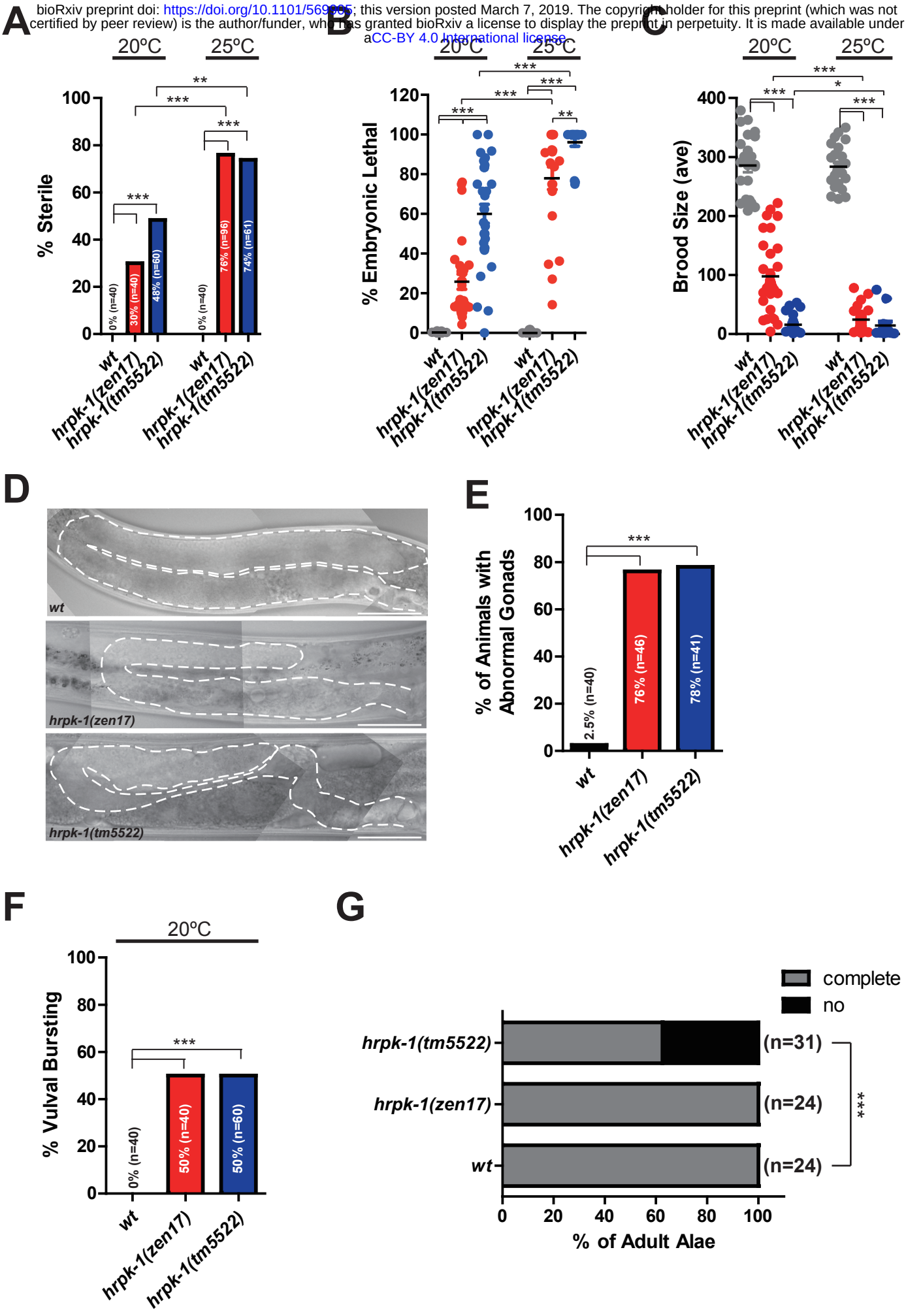

Figure 3

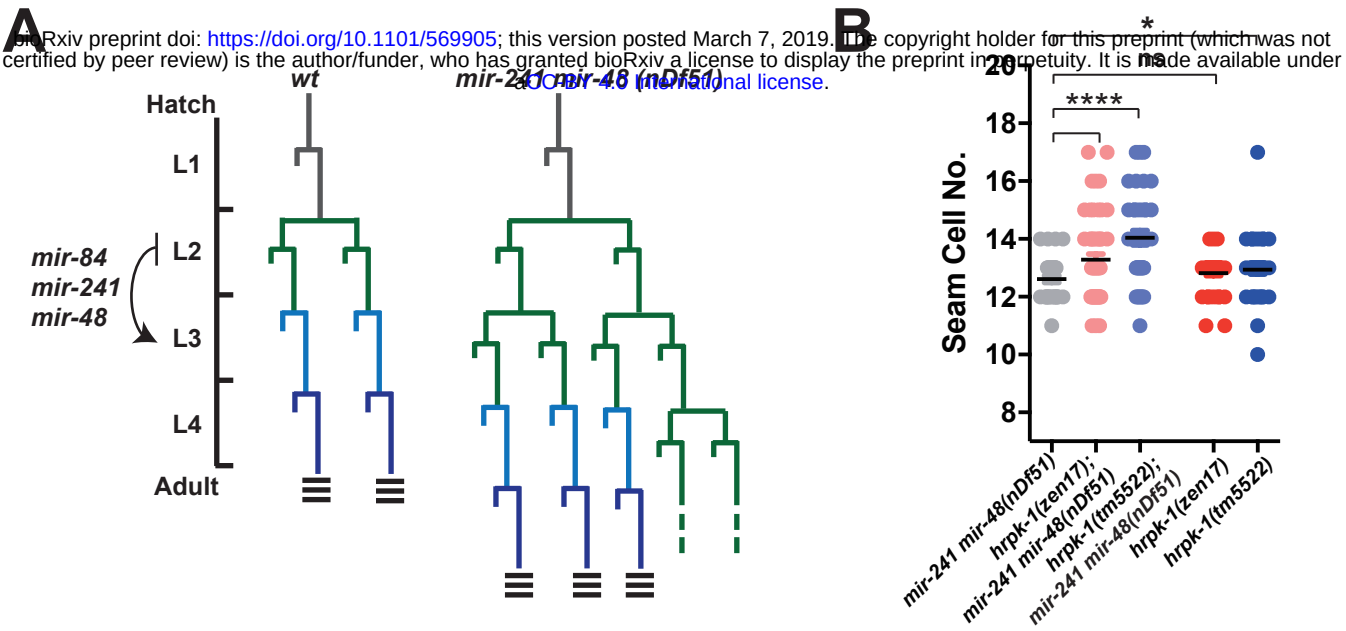

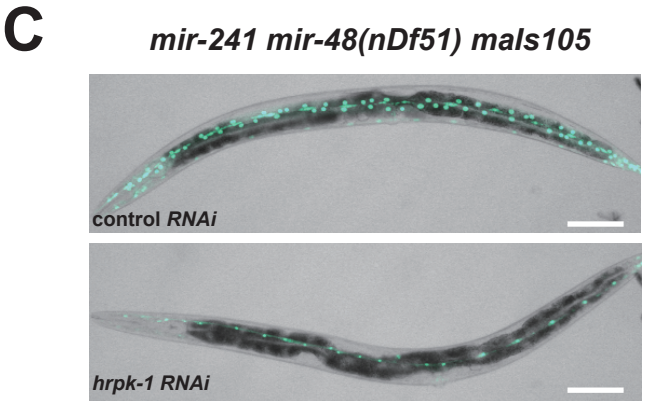

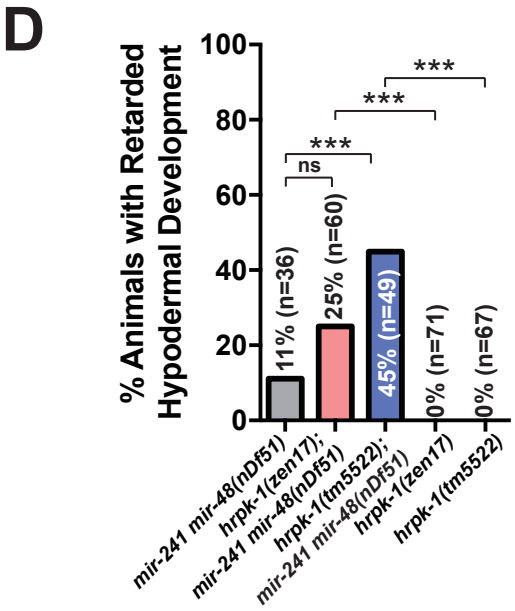

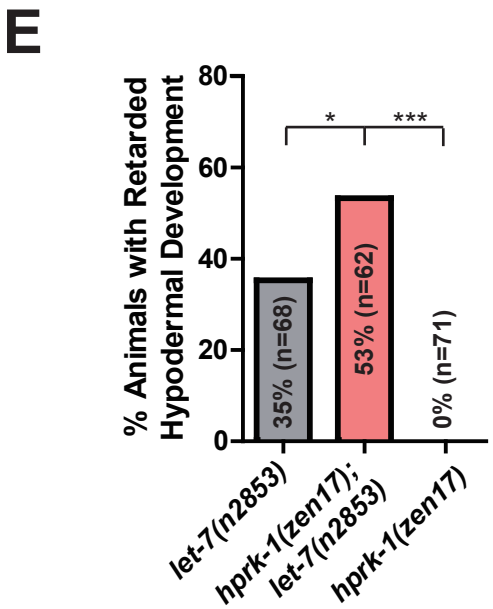

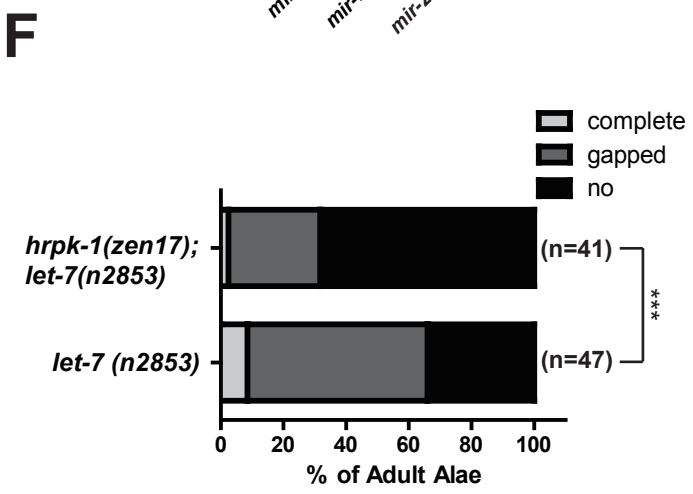

Figure 4

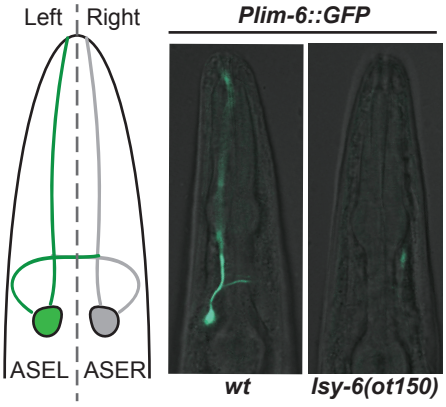

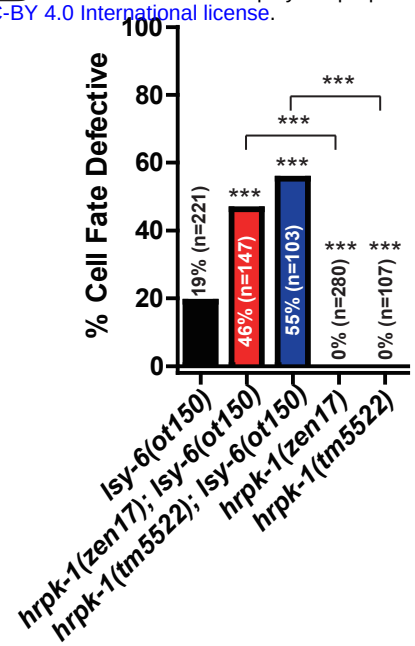

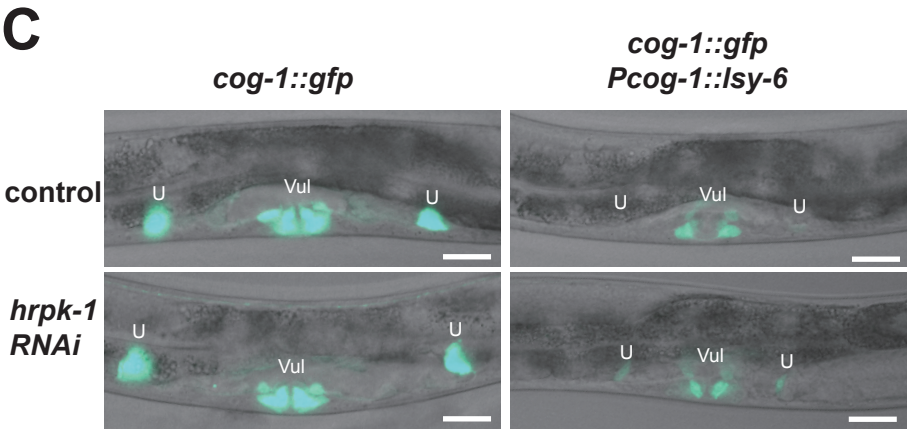

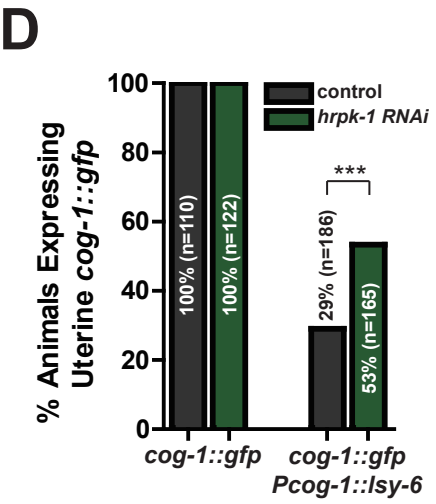

Figure 5

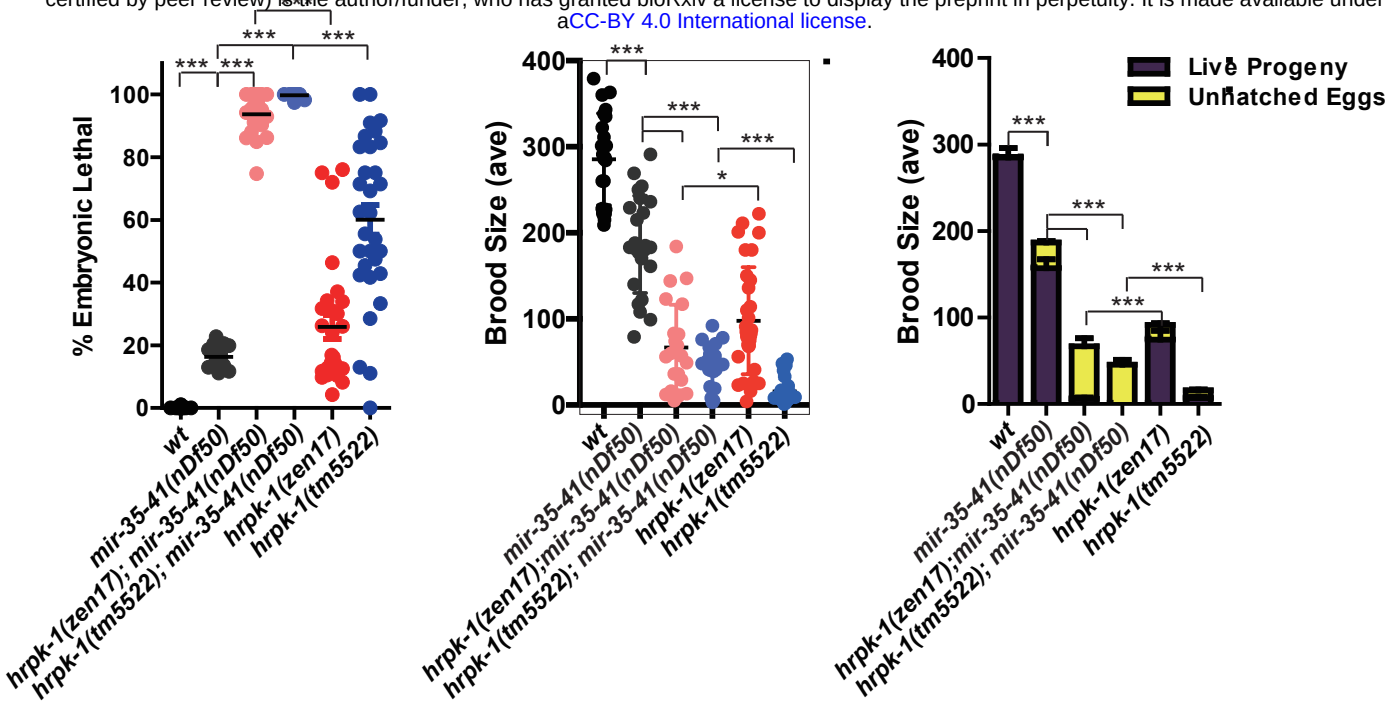

Figure 6

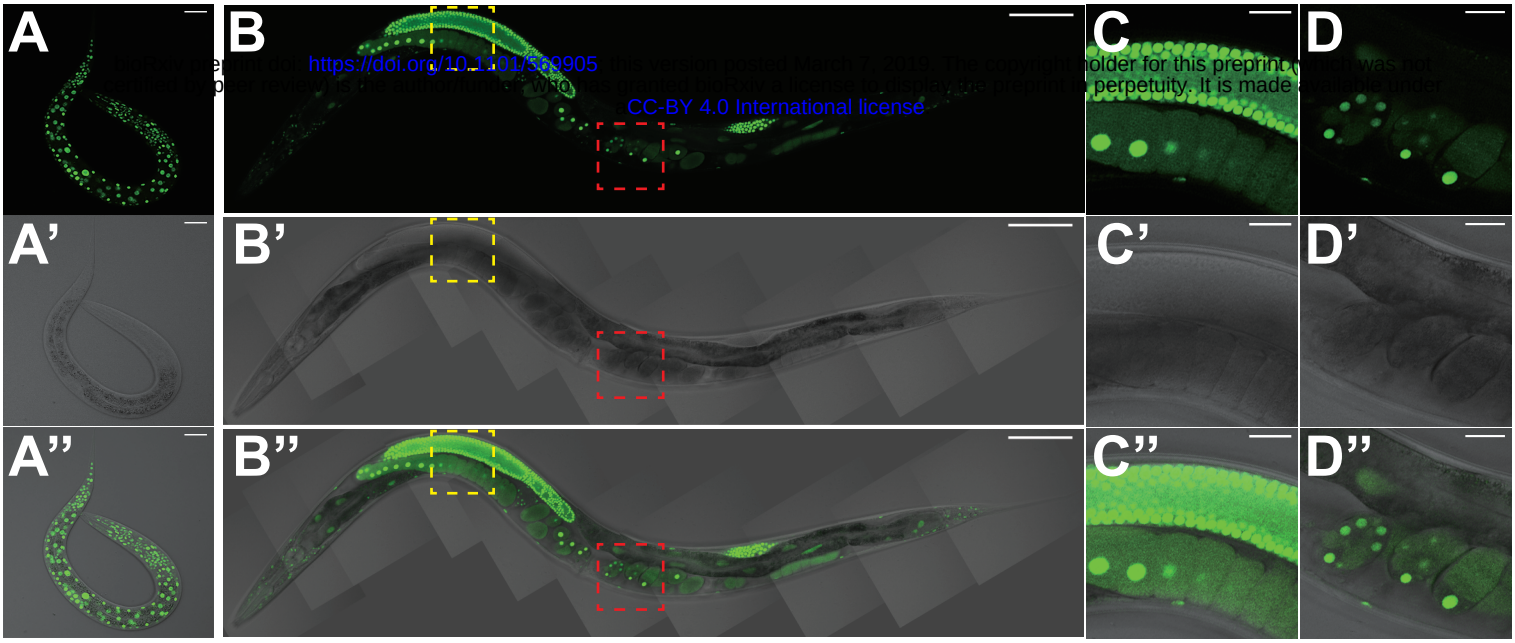

Figure 7

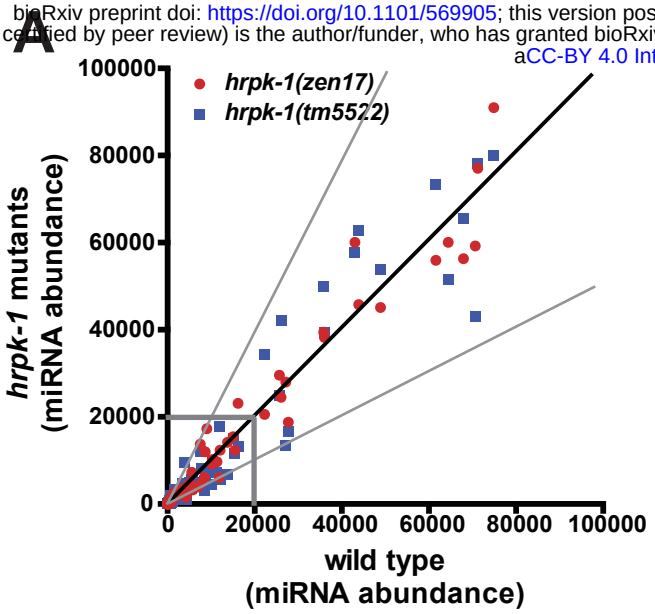

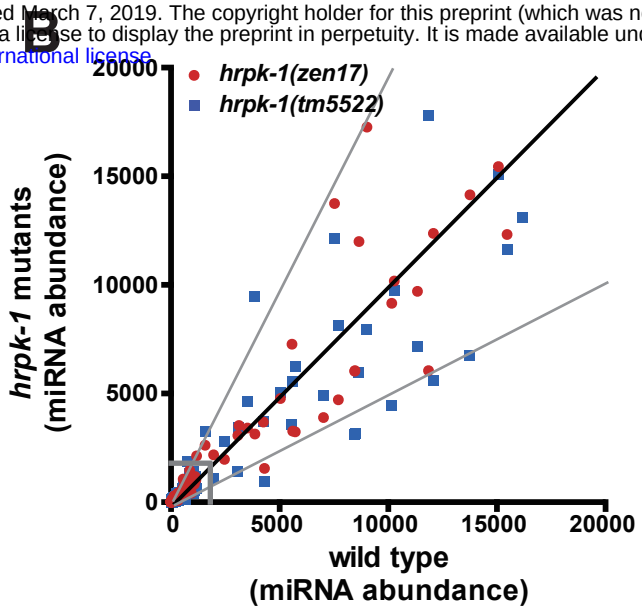

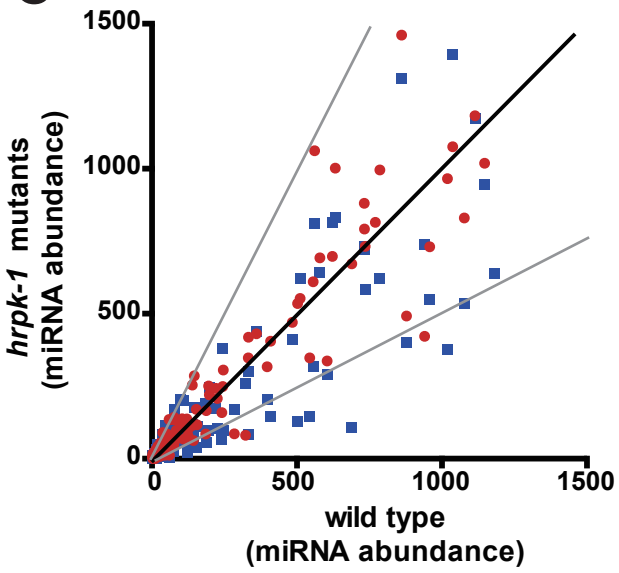

D

Average miRNA abundance (ppm)

	wild type	*hrpk-1 (zen17)*	*hrpk-1 (tm5522)*
mir-84	7533	13746	12134
let-7	16189	23121	13109
lsy-6	17	7	4
mir-42	1965	2178	1098

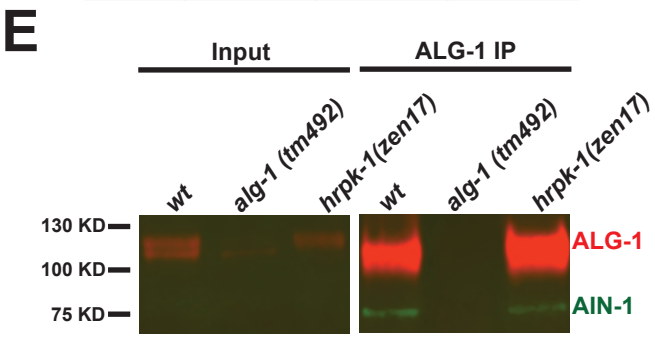

Figure 8

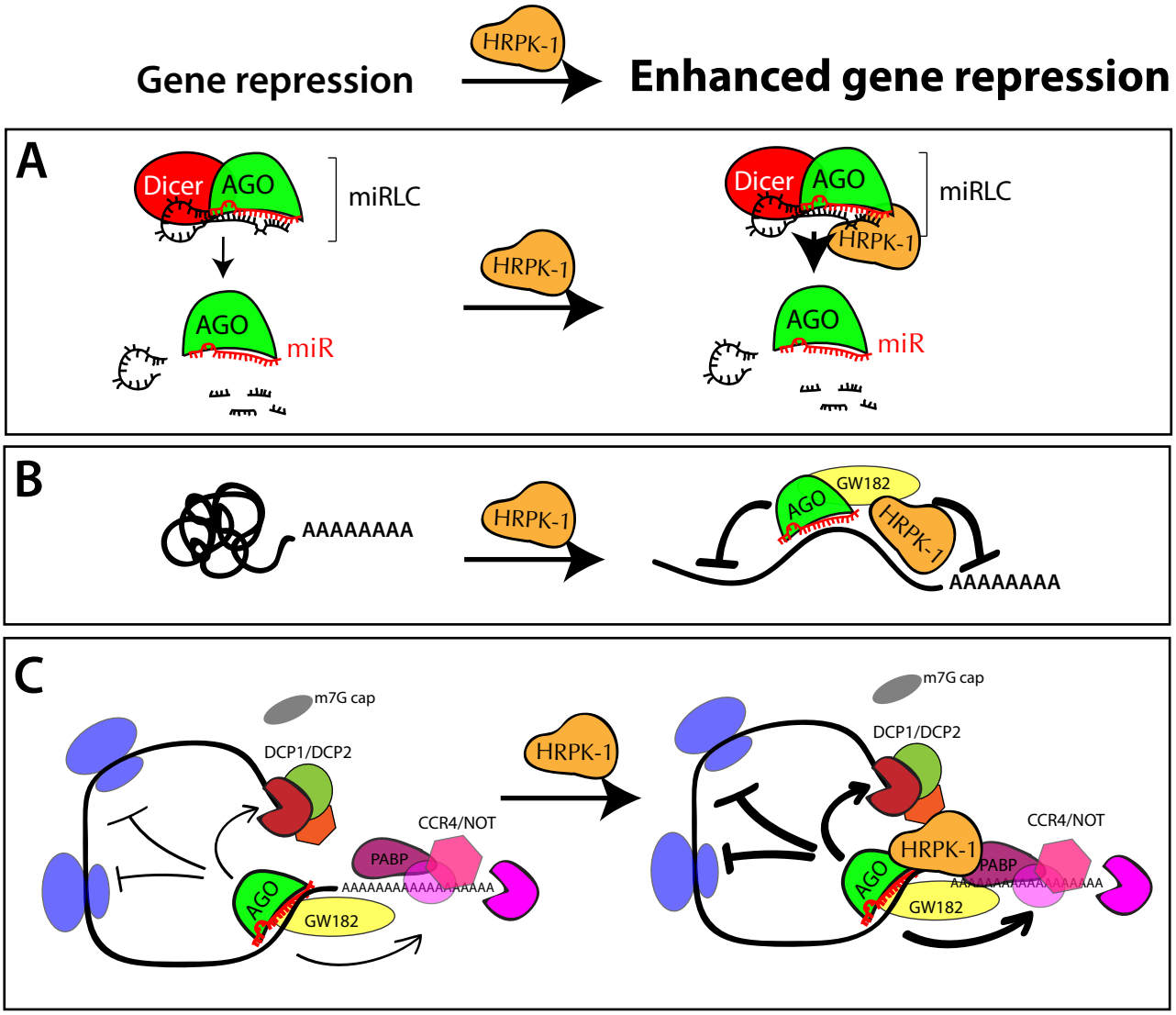

S1 Figure

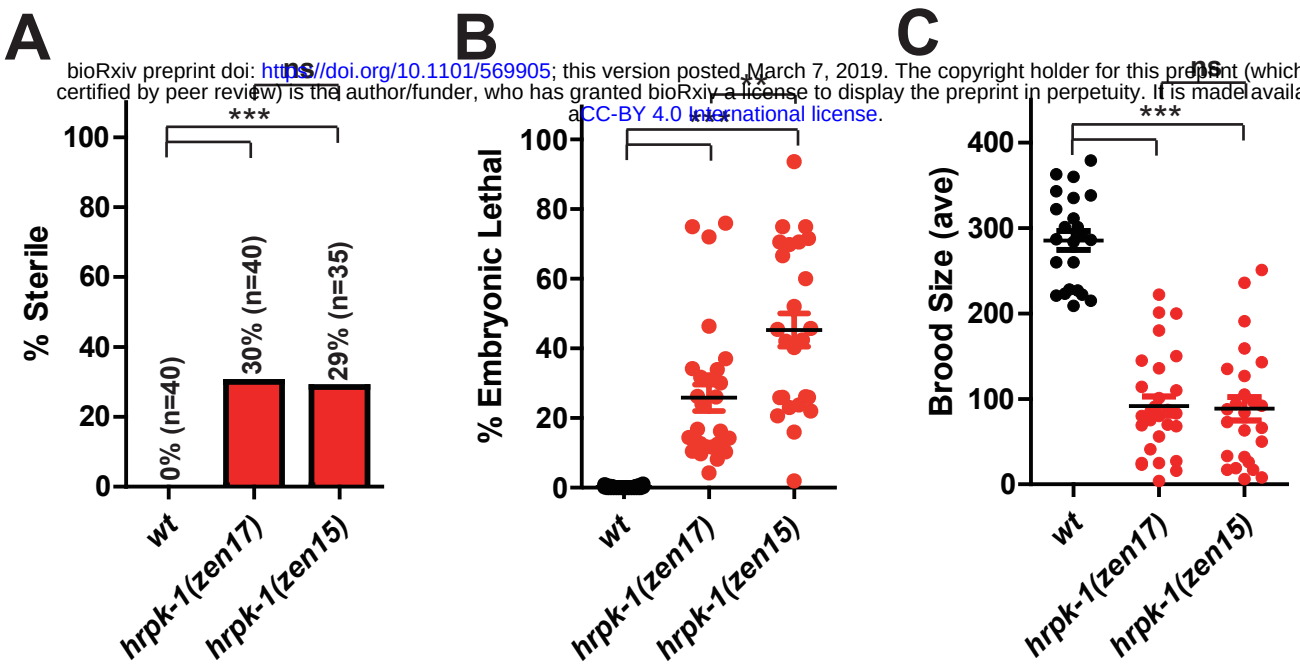

S2 Figure

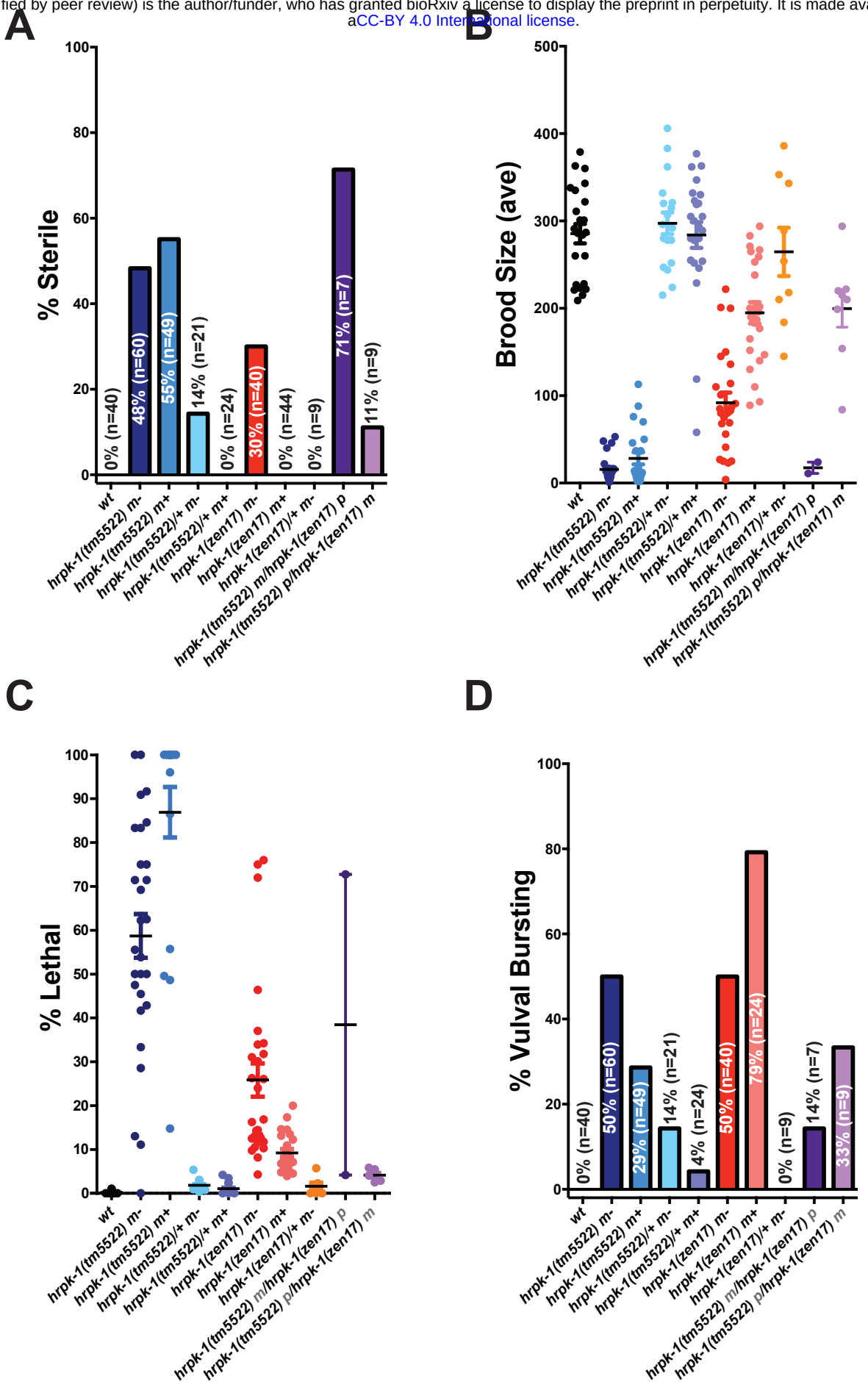

S3 Figure

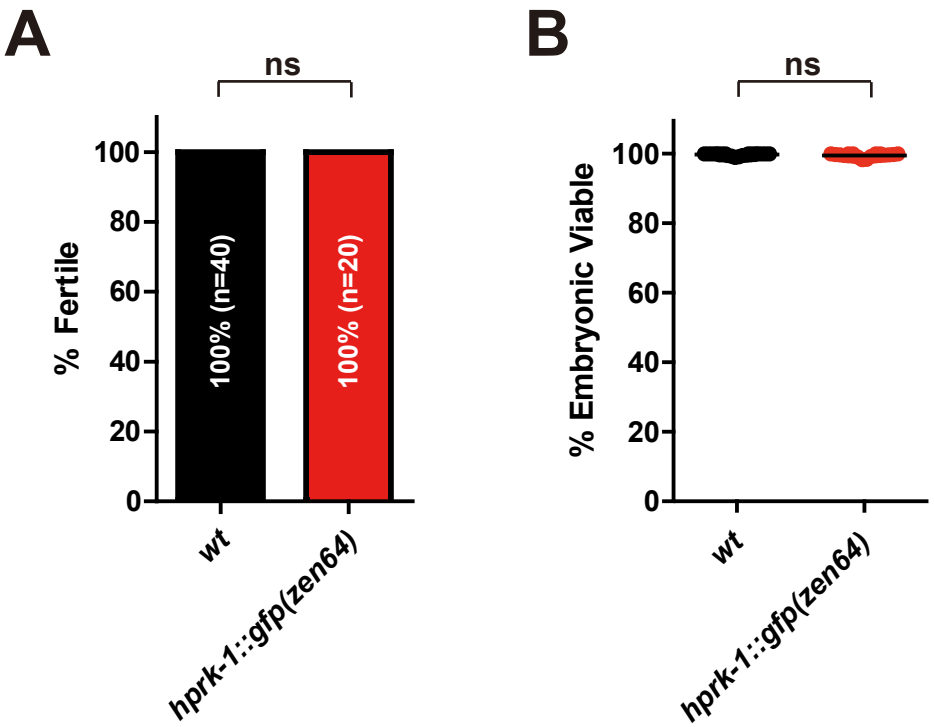

Table S1. miRNA abundances in *hrpk-1* mutants compared to wild type.

	Average ppm			miRNA abundance ratios	
	wild type (N2)	*hrpk-1(zen17)* (UY38)	*hrpk-1(tm5522)* (UY42)	N2/UY38	N2/UY42
cel-mir-1	74879	90996	79987	0.82288702	0.93613817
cel-mir-55	71238	77076	78063	0.92425548	0.91257553
cel-mir-58	70633	59249	43092	1.19214551	1.63912268
cel-mir-51	67946	56298	65614	1.20690154	1.03554933
cel-mir-81	64442	60042	51633	1.07328978	1.24807751
cel-mir-56	61610	55943	73417	1.10128263	0.83917441
cel-mir-82	48915	45119	53873	1.08413796	0.90796257
cel-mir-71	43901	45757	62856	0.95942636	0.69843458
cel-mir-48	43036	60043	57808	0.7167505	0.74445451
cel-mir-80	36004	38232	39455	0.94172811	0.91255007
cel-mir-228	35850	39421	49972	0.90940965	0.71740711
cel-mir-66	27717	18787	16615	1.47531147	1.66817059
cel-mir-77	27125	27999	13443	0.9687709	2.01783513
cel-mir-65	26047	24476	42037	1.06416156	0.61962331
cel-mir-238	25675	29573	25000	0.86818509	1.02701121
cel-mir-64	22258	20553	34319	1.08293925	0.64854969
cel-let-7	16189	23121	13109	0.70018187	1.23499237
cel-mir-72	15473	12322	11647	1.25569632	1.32841399
cel-mir-70	15068	15446	15075	0.97549638	0.99954244
cel-mir-47	13766	14143	6748	0.97339683	2.04017174
cel-mir-46	12081	12373	5615	0.97642156	2.151529
cel-mir-35	11855	6052	17811	1.95865723	0.66555654
cel-mir-52	11349	9700	7181	1.1699458	1.58043332
cel-mir-73	10281	10175	9744	1.01040939	1.05507938
cel-lin-4	10164	9152	4432	1.11059553	2.29338471
cel-mir-90	9023	17264	7931	0.52266835	1.13776012
cel-mir-60	8655	11998	5984	0.72134739	1.44616044
cel-mir-45	8470	6055	3158	1.39880858	2.68173132
cel-mir-44	8451	6030	3138	1.40136828	2.6930232
cel-mir-40	7706	4711	8118	1.63565648	0.94926702
cel-mir-84	7533	13746	12134	0.54804116	0.6208383
cel-mir-39	7022	3898	4887	1.80141274	1.43686287
cel-mir-61	5717	3237	6239	1.7659653	0.91636597
cel-mir-57	5604	3268	5561	1.71451512	1.00772486
cel-mir-54	5569	7267	3584	0.76641772	1.55411248
cel-mir-235	5037	4769	5040	1.05610328	0.9992189
cel-mir-86	4308	1557	963	2.7671303	4.47161407
cel-mir-241	4254	3684	3699	1.1548206	1.15026628
cel-mir-37	3866	3134	9446	1.23335545	0.40924066
cel-mir-237	3525	3413	4627	1.03289653	0.76176232
cel-mir-786	3128	3533	3436	0.88543597	0.91046376
cel-mir-87	3077	3069	1399	1.00261707	2.19839806
cel-mir-63	2464	1975	2786	1.24726112	0.88433149
cel-mir-42	1965	2178	1098	0.90208355	1.78916649
cel-mir-246	1568	2621	3251	0.59820068	0.48229869
cel-mir-229	1180	2130	640	0.55406263	1.84423182
cel-mir-49	1147	1019	946	1.12576048	1.21351998
cel-mir-234	1114	1183	1173	0.94151039	0.94927049
cel-mir-233	1077	830	536	1.29750966	2.00949259
cel-mir-50	1037	1076	1395	0.96322329	0.74324465
cel-mir-79	1019	966	377	1.0547668	2.69876083
cel-mir-253	940	422	739	2.2291931	1.2725538
cel-mir-36	878	492	401	1.78722865	2.19066898
cel-mir-252	861	1461	1312	0.58916541	0.65589185
cel-mir-83	786	996	621	0.7887272	1.26530483
cel-mir-85	770	815	1858	0.94487194	0.41471926
cel-mir-248	732	881	722	0.83032462	1.01421948
cel-mir-62	689	672	109	1.02577066	6.31759044
cel-mir-240	632	1002	830	0.63104118	0.76197712
cel-mir-230	622	698	816	0.8909715	0.76243954
cel-mir-76	561	1062	813	0.52789379	0.69002724
cel-mir-59	556	610	319	0.91244159	1.74122477
cel-mir-2	544	348	144	1.56332608	3.77469109
cel-mir-790	511	553	621	0.92332733	0.82251599
cel-mir-236	502	535	128	0.93719175	3.91417986
cel-mir-53	484	470	410	1.03078621	1.18031902
cel-mir-74	397	317	206	1.25468958	1.92595893
cel-mir-67	332	348	83	0.95534244	3.98952192
cel-mir-250	284	86	170	3.3078772	1.66855663
cel-mir-785	244	249	381	0.97769935	0.64070416
cel-mir-41	241	159	65	1.51947757	3.73772109
cel-mir-259	225	208	104	1.0807678	2.16148981
cel-mir-243	220	243	172	0.90434837	1.27915526
cel-mir-793	198	220	245	0.89822072	0.80710781
cel-mir-1817	195	251	97	0.77797642	2.01602989
cel-mir-34	155	117	111	1.32837851	1.40336829
cel-mir-355	146	286	177	0.51106063	0.82306027
cel-mir-244	120	137	58	0.87289515	2.06802355
cel-mir-1022	110	109	105	1.00510508	1.04712525
cel-mir-78	109	68	200	1.605736	0.54375324
cel-mir-359	104	138	135	0.75714873	0.77035472
cel-mir-245	97	133	205	0.730466	0.47147436
cel-mir-356b	97	109	58	0.88888344	1.65939462
cel-mir-4816	84	98	74	0.85673074	1.13399894
cel-mir-1829c	82	88	110	0.93803448	0.74455755
cel-mir-788	78	82	124	0.95373938	0.63110879
cel-mir-5592-2	76	143	114	0.52906579	0.66359477
cel-mir-124	74	47	25	1.57115552	2.9243556
cel-mir-232	68	52	43	1.2978008	1.58860264
cel-mir-789-1	66	45	49	1.4590919	1.33495437
cel-mir-75	63	65	42	0.96639591	1.51092629
cel-mir-38	63	45	60	1.39323167	1.05260548
cel-mir-799	61	63	30	0.97880631	2.01615828
cel-mir-231	61	40	31	1.52848588	1.96081986
cel-mir-1829a	51	86	61	0.58751802	0.82567588
cel-mir-797	48	36	21	1.33324354	2.28559955
cel-mir-1020	48	49	48	0.97532677	0.98865418
cel-mir-1820	46	65	116	0.70446825	0.39813318
cel-mir-358	46	46	12	1.00693492	3.72329015
cel-mir-787	42	44	53	0.95875023	0.7968975
cel-mir-784	42	46	60	0.91275316	0.70693198
cel-mir-357	42	33	49	1.28159608	0.85485674
cel-mir-239a	38	54	32	0.69879122	1.16889096
cel-mir-795	37	90	84	0.41329344	0.44449125
cel-mir-247	30	18	11	1.70899097	2.7072559
cel-mir-1819	29	54	41	0.54332384	0.70822515
cel-mir-5551	20	16	19	1.26376292	1.10232952
cel-mir-254	20	30	50	0.67392918	0.40279933
cel-mir-1821	20	43	48	0.4610015	0.4124488
cel-mir-255	18	32	16	0.57459602	1.17999387
cel-mir-4813	18	17	7	1.05873009	2.58102992
cel-lsy-6	17	7	4	2.2788856	4.50449923
cel-mir-1824	17	15	1	1.0759907	12.7771334
cel-mir-791	13	30	17	0.45017175	0.78193564
cel-mir-249	13	19	19	0.70114113	0.68924337
cel-mir-242	13	12	9	1.06972891	1.48016817
cel-mir-798	11	0	6	37.6433551	1.92694407
cel-mir-4937	9	4	0	2.60959102	47.5636922
cel-mir-1822	9	10	11	0.87968359	0.79158764
cel-mir-794	8	11	7	0.75423876	1.19006147
cel-mir-1830	8	9	7	0.88678844	1.05218454
cel-mir-796	7	7	18	0.91537225	0.37449794
cel-mir-4808	7	6	8	1.0979629	0.80406727
cel-mir-260	7	4	0	1.68086486	#DIV/0!
cel-mir-4814	6	6	0	1.01747292	38.7210439
cel-mir-4920	6	5	0	1.12373573	#DIV/0!
cel-mir-2212	5	5	0	1.01663464	#DIV/0!
cel-mir-4929	5	2	0	2.16784438	#DIV/0!
cel-mir-2214	4	3	2	1.54229843	2.54193881
cel-mir-43	4	8	5	0.48034199	0.81808972
cel-mir-2210	4	10	8	0.38792361	0.45955438
cel-mir-4936	4	2	12	1.97952772	0.30270965
cel-mir-800	3	4	2	0.8745579	2.27594634
cel-mir-4807	3	1	8	2.90363522	0.44508557
cel-mir-239b	3	10	0	0.33758423	10.3418473
cel-mir-2209a	3	7	13	0.4770511	0.25906633

Table S2. Mature miRNAs whose abundance was changed 2-fold or more in *hrpk-1* mutants compared to wild type.

miRNAs with ≥2-fold decreased abundance are highlighted in gray. miRNAs whose abundace increased in *hrpk-1* mutants ≥2-fold are highlighted in blue.

	wild type (N2)	*hrpk-1(zen17)* (UY38)	*hrpk-1(tm5522)* (UY42)	N2/UY38 Ratio	N2/UY42 Ratio
cel-mir-798	11	0	6	37.643	1.927
cel-mir-250	284	86	170	3.308	1.669
cel-mir-86	4308	1557	963	2.767	4.472
cel-lsy-6	17	7	4	2.279	4.504
cel-mir-253	940	422	739	2.229	1.273
cel-mir-36	878	492	401	1.787	2.191
cel-mir-247	30	18	11	1.709	2.771
cel-mir-124	74	47	25	1.571	2.924
cel-mir-2	544	348	144	1.563	3.775
cel-mir-41	241	159	65	1.519	3.738
cel-mir-44	8451	6030	3138	1.401	2.693
cel-mir-45	8470	6055	3158	1.399	2.682
cel-mir-797	48	36	21	1.333	2.286
cel-mir-233	1077	830	536	1.298	2.009
cel-lin-4	10164	9152	4432	1.111	2.293
cel-mir-259	225	208	104	1.081	2.161
cel-mir-1824	17	15	1	1.076	12.777
cel-mir-4813	18	17	7	1.059	2.581
cel-mir-79	1019	966	377	1.055	2.699
cel-mir-62	689	672	109	1.026	6.318
cel-mir-47	409	405	145	1.010	2.817
cel-mir-358	46	46	12	1.007	3.723
cel-mir-87	3077	3069	1399	1.003	2.198
cel-mir-799	61	63	30	0.979	2.016
cel-mir-47	13766	14143	6748	0.973	2.040
cel-mir-77	27125	27999	13443	0.969	2.018
cel-mir-67	332	348	83	0.955	3.990
cel-mir-236	502	535	128	0.937	3.914
cel-mir-244	120	137	58	0.873	2.068
cel-mir-1817	195	251	97	0.778	2.016
cel-mir-245	97	133	205	0.730	0.471
cel-mir-1820	46	65	116	0.704	0.398
cel-mir-254	20	30	50	0.674	0.403
cel-mir-246	1568	2621	3251	0.598	0.482
cel-mir-1821	20	43	48	0.461	0.412
cel-mir-791	13	30	17	0.450	0.782
cel-mir-795	37	90	84	0.413	0.444
cel-mir-37	3866	3134	9446	1.233	0.409